“凝聚态物理–北京大学论坛”
Forum on condensed matter physics at PKU
2014

为什么是 MoS_2？

报告人 吕劲

北京大学物理学院
人工微结构与介观物理国家重点实验室
量子物质科学协同创新中心
2014 年10月30日

纳米材料按照维度的发展

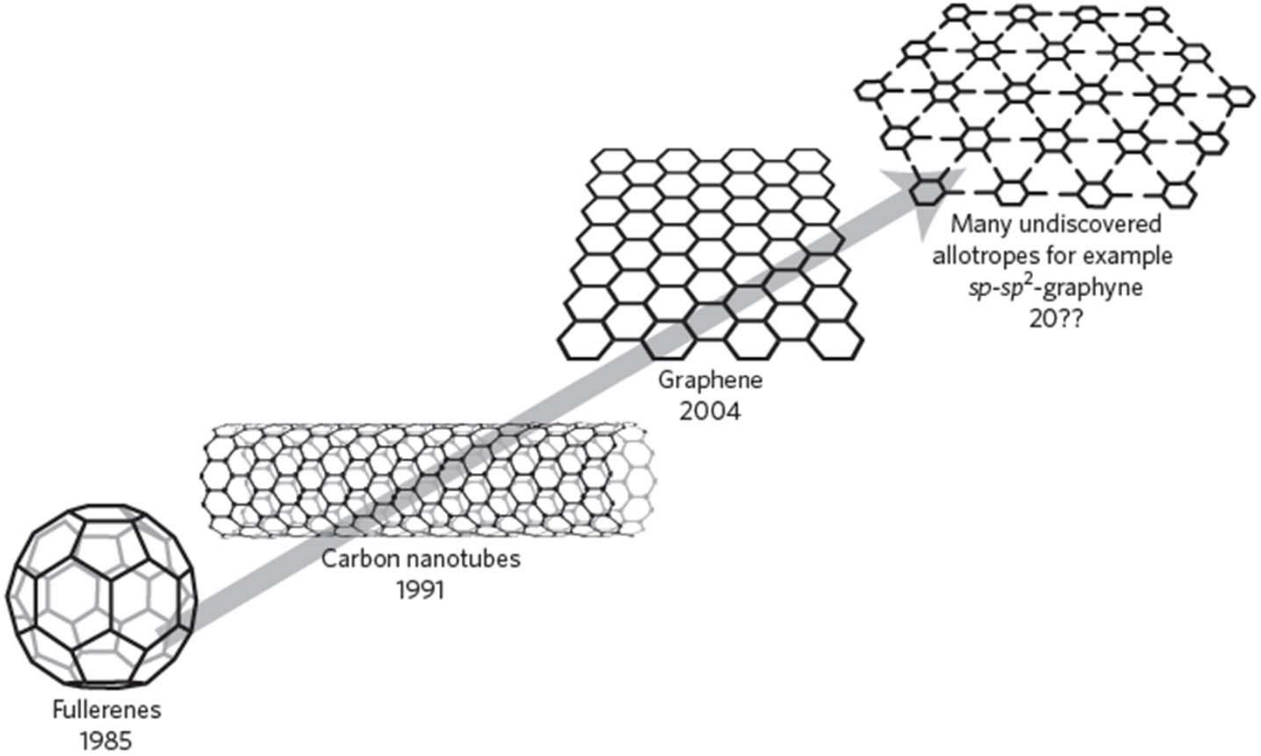

与三维块材，零维的团簇，一维的纳米线和管，二维材料是人认识最少的维度材料

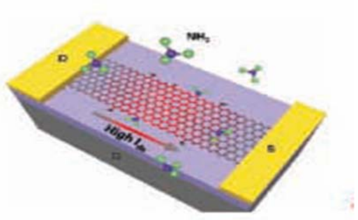

最大的表面积，高的探测效率

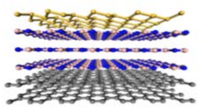

用堆积造出新的结构

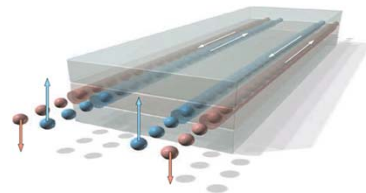

2D的拓扑绝缘体
可以有量子自旋
霍尔效应
反常量子霍尔效应

2D 材料
石墨烯，BN， 硅烯，石墨炔，
MoS_2

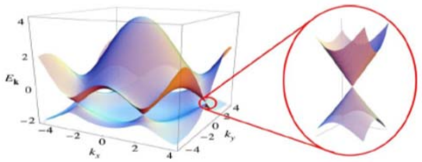

狄拉克锥 非常高的载流子迁移率 快速装置

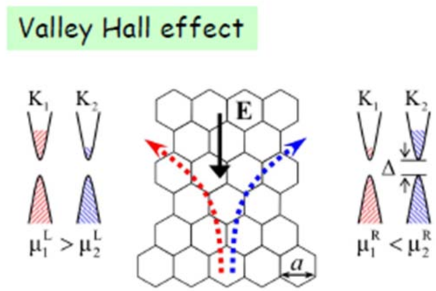

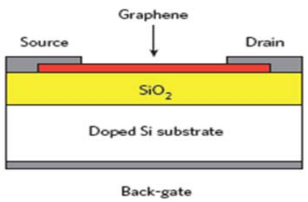

做场效应管 短沟道效应受抑制

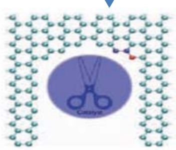

平面结构易于
加工成需要的平板电路

基本检索 | 作者检索 | 被引参考文献检索 | 化学结构检索 | 高级检索 | 检索历史

Web of Science®

检索结果 出版年=(2012) AND 出版物名称=(nature nanotechnology)
时间跨度=所有年份。 数据库=SCI-EXPANDED, SSCI, A&HCI, CPCI-S, CPCI-SSH, CCR-EXPANDED, IC。
创建跟踪 / RSS

检索结果: 197 | 第 1 页，共 20 页 转至 | 排序方式: 被引频次 (降序)

分析检索结果
创建引文报告

精炼检索结果

结果内检索 [检索]

▼ Web of Science 类别 [精炼]
- MATERIALS SCIENCE MULTIDISCIPLINARY (197)
- NANOSCIENCE NANOTECHNOLOGY (197)

更多选项/分类…

▼ 文献类型 [精炼]
- ARTICLE (115)
- NEWS ITEM (56)
- EDITORIAL MATERIAL (9)
- CORRECTION (7)
- REVIEW (6)

更多选项/分类…

- ► 研究方向
- ► 作者
- ► 团体作者
- ► 编者
- ► 来源出版物
- ► 丛书名称
- ► 会议名称
- ► 出版年
- ► 机构扩展
- ► 基金资助机构
- ► 语种
- ► 国家/地区

要获得更多精炼选项，请使用
分析检索结果

选择页面 | 添加到标记结果列表 (0) | 发送到: my.endnote.com

1. 标题: Electronics and optoelectronics of two-dimensional transition metal dichalcogenides
作者: Wang, Qing Hua; Kalantar-Zadeh, Kourosh; Kis, Andras; 等.
来源出版物: NATURE NANOTECHNOLOGY 卷: 7 期: 11 页: 699-712 DOI: 10.1038/NNANO.2012.193 出版年: NOV 2012
被引频次: 149 (来自 Web of Science)
全文 | LINK @PKUL | [查看摘要]

2. 标题: Stable cycling of double-walled silicon nanotube battery anodes through solid-electrolyte interphase control
作者: Wu, Hui; Chan, Gerentt; Choi, Jang Wook; 等.
来源出版物: NATURE NANOTECHNOLOGY 卷: 7 期: 5 页: 309-314 DOI: 10.1038/NNANO.2012.35 出版年: MAY 2012
被引频次: 126 (来自 Web of Science)
全文 | LINK @PKUL | [查看摘要]

3. 标题: Control of valley polarization in monolayer MoS2 by optical helicity
作者: Mak, Kin Fai; He, Keliang; Shan, Jie; 等.
来源出版物: NATURE NANOTECHNOLOGY 卷: 7 期: 8 页: 494-498 DOI: 10.1038/NNANO.2012.96 出版年: AUG 2012
被引频次: 121 (来自 Web of Science)
全文 | LINK @PKUL | [查看摘要]

4. 标题: Valley polarization in MoS2 monolayers by optical pumping
作者: Zeng, Hualing; Dai, Junfeng; Yao, Wang; 等.
来源出版物: NATURE NANOTECHNOLOGY 卷: 7 期: 8 页: 490-493 DOI: 10.1038/NNANO.2012.95 出版年: AUG 2012
被引频次: 118 (来自 Web of Science)
全文 | LINK @PKUL | [查看摘要]

5. 标题: The properties and applications of nanodiamonds
作者: Mochalin, Vadym N.; Shenderova, Olga; Ho, Dean; 等.
来源出版物: NATURE NANOTECHNOLOGY 卷: 7 期: 1 页: 11-23 DOI: 10.1038/NNANO.2011.209 出版年: JAN 2012
被引频次: 113 (来自 Web of Science)
全文 | LINK @PKUL | [查看摘要]

6. 标题: Tunable infrared plasmonic devices using graphene/insulator stacks
作者: Yan, Hugen; Li, Xuesong; Chandra, Bhupesh; 等.
来源出版物: NATURE NANOTECHNOLOGY 卷: 7 期: 5 页: 330-334 DOI: 10.1038/NNANO.2012.59 出版年: MAY 2012
被引频次: 95 (来自 Web of Science)
全文 | LINK @PKUL | [查看摘要]

7. 标题: An oxygen reduction electrocatalyst based on carbon nanotube-graphene complexes
作者: Li, Yanguang; Zhou, Wu; Wang, Hailiang; 等.
来源出版物: NATURE NANOTECHNOLOGY 卷: 7 期: 6 页: 394-400 DOI: 10.1038/NNANO.2012.72 出版年: JUN 2012
被引频次: 90 (来自 Web of Science)
全文 | LINK @PKUL | [查看摘要]

8. 标题: A single-atom transistor
作者: Fuechsle, Martin; Miwa, Jill A.; Mahapatra, Suddhasatta; 等.
来源出版物: NATURE NANOTECHNOLOGY 卷: 7 期: 4 页: 242-246 DOI: 10.1038/NNANO.2012.21 出版年: APR 2012
被引频次: 79 (来自 Web of Science)
全文 | LINK @PKUL | [查看摘要]

9. 标题: Transport spectroscopy of symmetry-broken insulating states in bilayer graphene
作者: Velasco, J., Jr.; Jing, L.; Bao, W.; 等.
来源出版物: NATURE NANOTECHNOLOGY 卷: 7 期: 3 页: 156-160 DOI: 10.1038/NNANO.2011.251 出版年: MAR 2012
被引频次: 78 (来自 Web of Science)
全文 | LINK @PKUL | [查看摘要]

10. 标题: Hybrid passivated colloidal quantum dot solids
作者: Ip, Alexander H.; Thon, Susanna M.; Hoogland, Sjoerd; 等.
来源出版物: NATURE NANOTECHNOLOGY 卷: 7 期: 9 页: 577-582 DOI: 10.1038/NNANO.2012.127 出版年: SEP 2012
被引频次: 72 (来自 Web of Science)
全文 | LINK @PKUL | [查看摘要]

选择页面 | 添加到标记结果列表 (0) | 发送到: my.endnote.com

检索结果: 197 每页显示 10 条 | 第 1 页，共 20 页 转至 | 排序方式: 被引频次 (降序)

您选择的数据限制内共有 51,609,549 条记录，其中有 197 条记录与检索式相匹配。
关键字: = 可用的化学结构。

查看: | 简体中文 | 繁體中文 | English | 日本語 | 한국어 | Português | Español

1　　电子结构

2D transition metal dichalcogenides

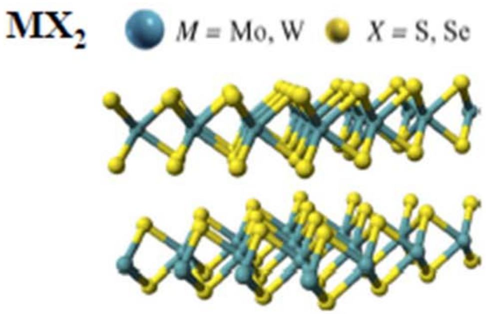

Layered structure suitable for extracting monolayer by mechanical exfoliation

Top view

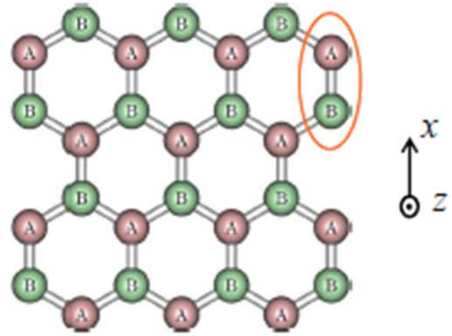

Bulk or even-layers

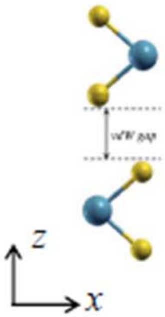

Indirect bandgap

with inversion symmetry

Even-odd oscillation of SHG
Zeng, et al. Sci Rep 13"

Monolayer

Direct bandgap

without inversion symmetry

Splendiani et al., NL 10"
Mak et al., PRL 10"

层数依赖

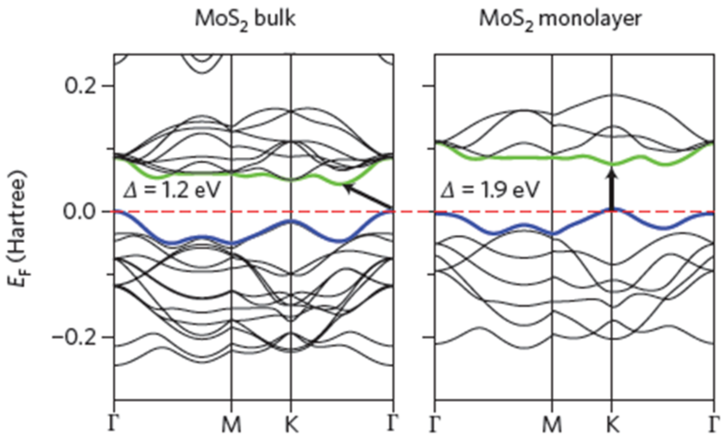

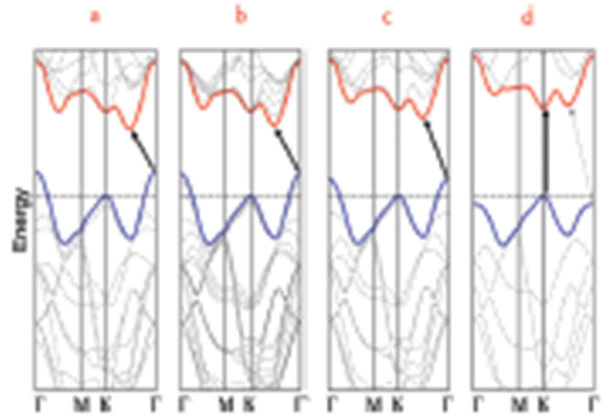

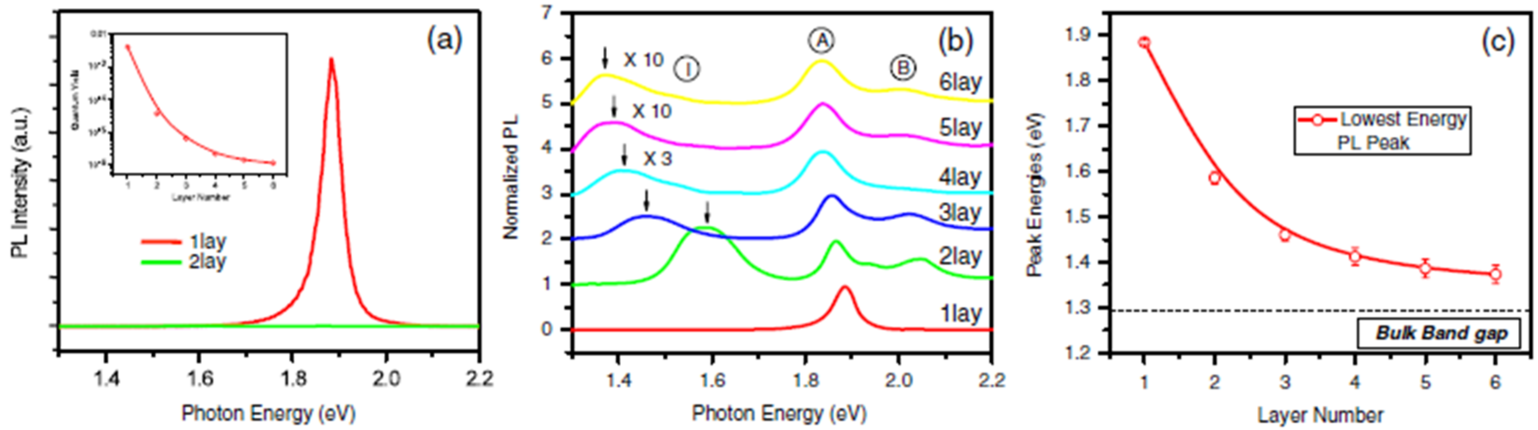

FIG. 3 (color online). (a) PL spectra for mono- and bilayer MoS_2 samples in the photon energy range from 1.3 to 2.2 eV. Inset: PL QY of thin layers for $N = 1$–6. (b) Normalized PL spectra by the intensity of peak A of thin layers of MoS_2 for $N = 1$–6. Feature I for $N = 4$–6 is magnified and the spectra are displaced for clarity. (c) Band-gap energy of thin layers of MoS_2, inferred from the energy of the PL feature I for $N = 2$–6 and from the energy of the PL peak A for $N = 1$. The dashed line represents the (indirect) band-gap energy of bulk MoS_2.

强烈的自旋轨道耦合

$$H_{SO} = \frac{g\mu_B}{2c^2}(\mathbf{v} \times \mathbf{E}) \cdot \sigma, \qquad \mathbf{B} = (\mathbf{v} \times \mathbf{E})/c^2,$$

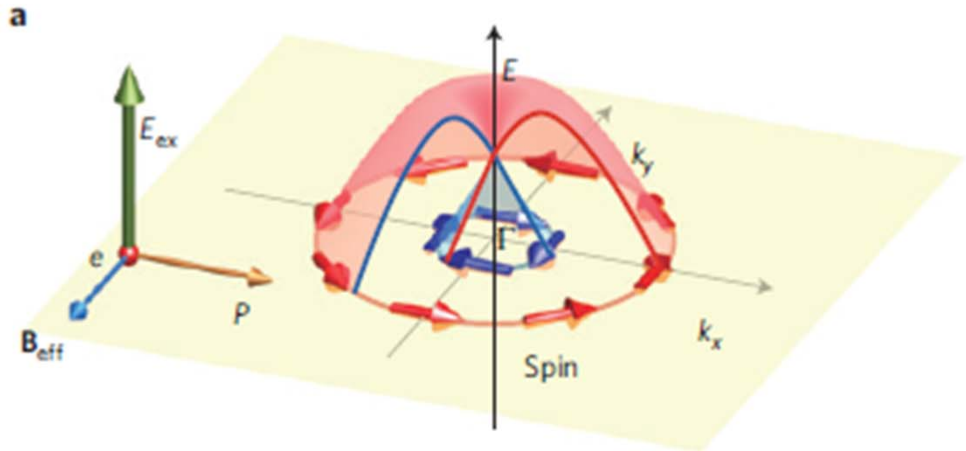

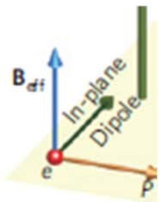

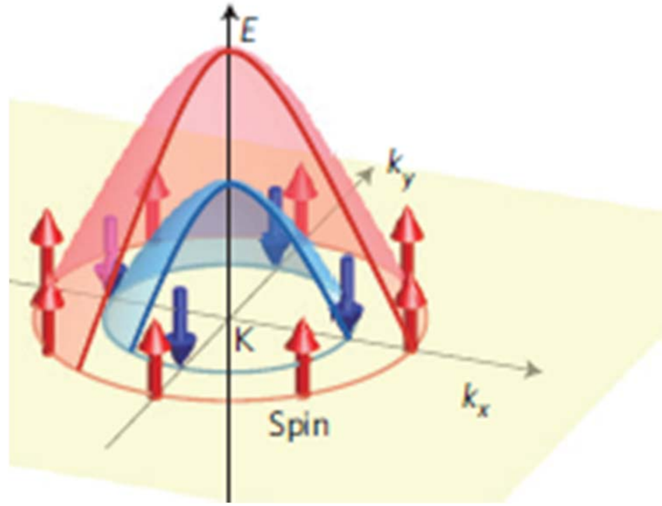

Monolayer group VIB TMDCs

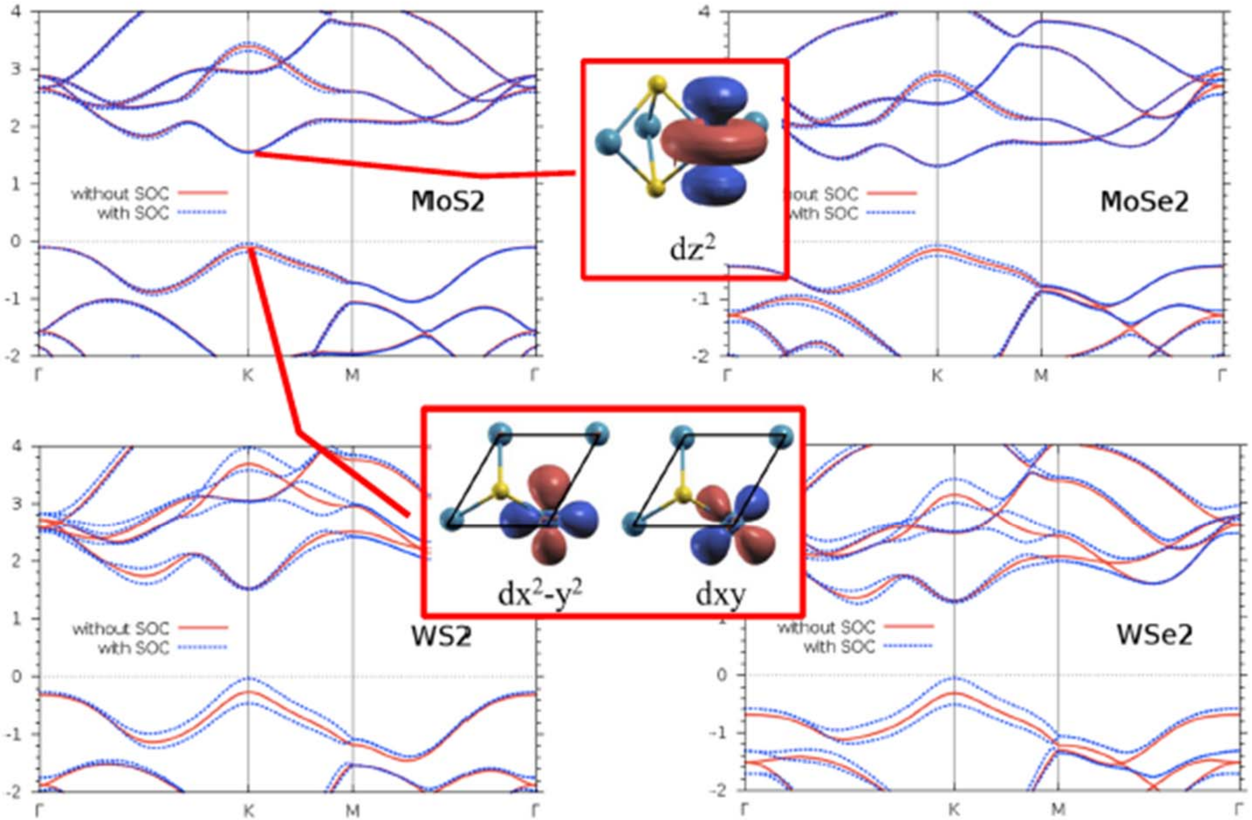

自旋轨道耦合的层数依赖的能带

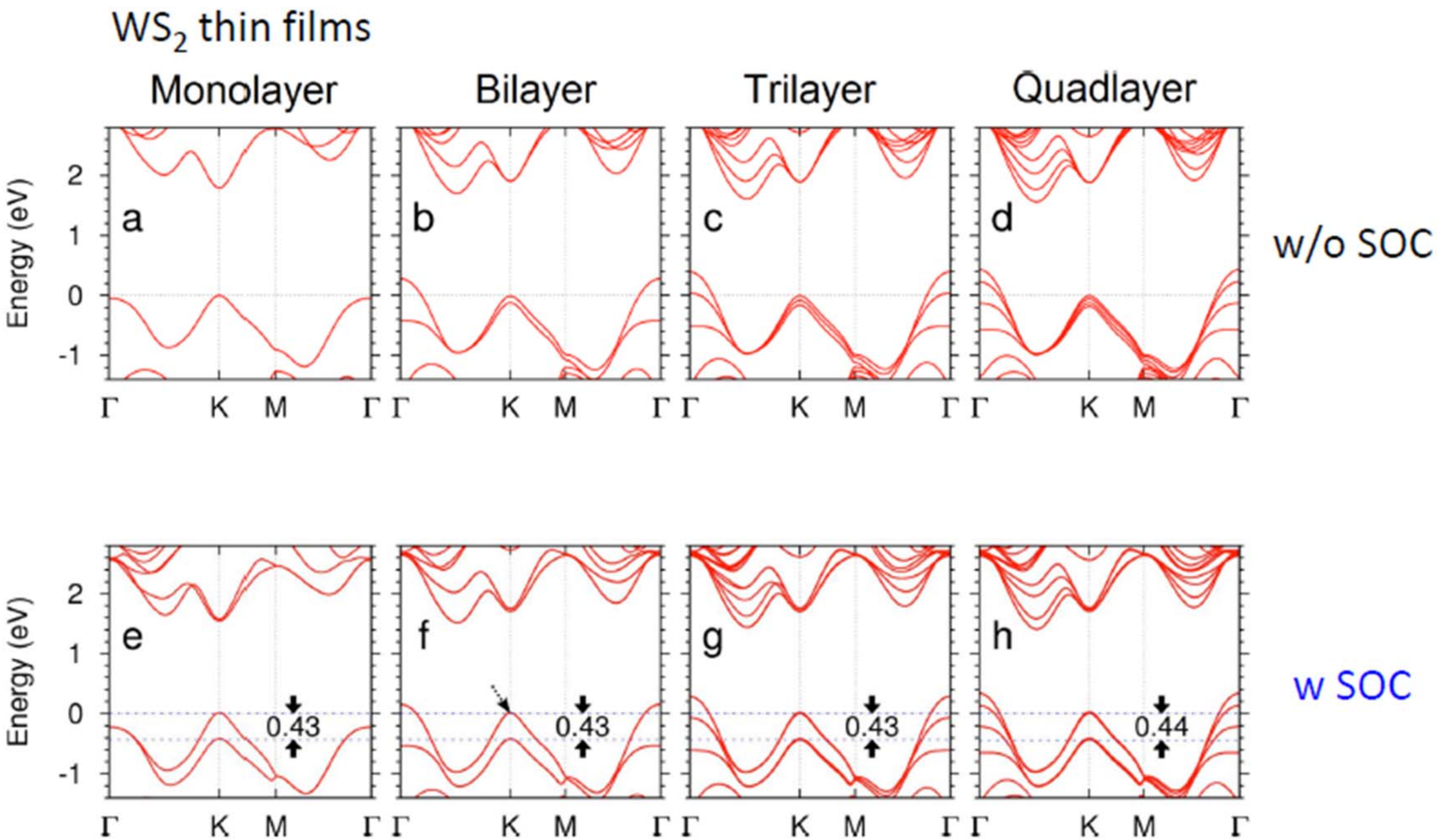

Zeng, Liu, et al. Scientific Reports 3, 168 (2013)

DFT

$$[-\frac{\nabla^2}{2} + V_{ion} + V_{Hartree} + v_{xc}[\rho(\boldsymbol{r})]]\psi_{nk} = E_{nk}\psi_{nk}$$

LDA 单做电子近似，与实验值比起，通常低估能隙 30-50%，
考虑多体效应可以有效修正

低维系统　　电子较少，屏蔽减弱，电子间库仑作用增强，多体效应更加明显
能带修正更大

GW------ 准粒子方法（G 格林函数，W屏蔽作用）

$$[-\frac{\nabla^2}{2} + V_{ion} + V_{Hartree} + \Sigma(E_{nk})]\psi_{nk} = E_{nk}\psi_{nk}$$

$$\Sigma = iGW$$

（G 格林函数，W屏蔽作用）

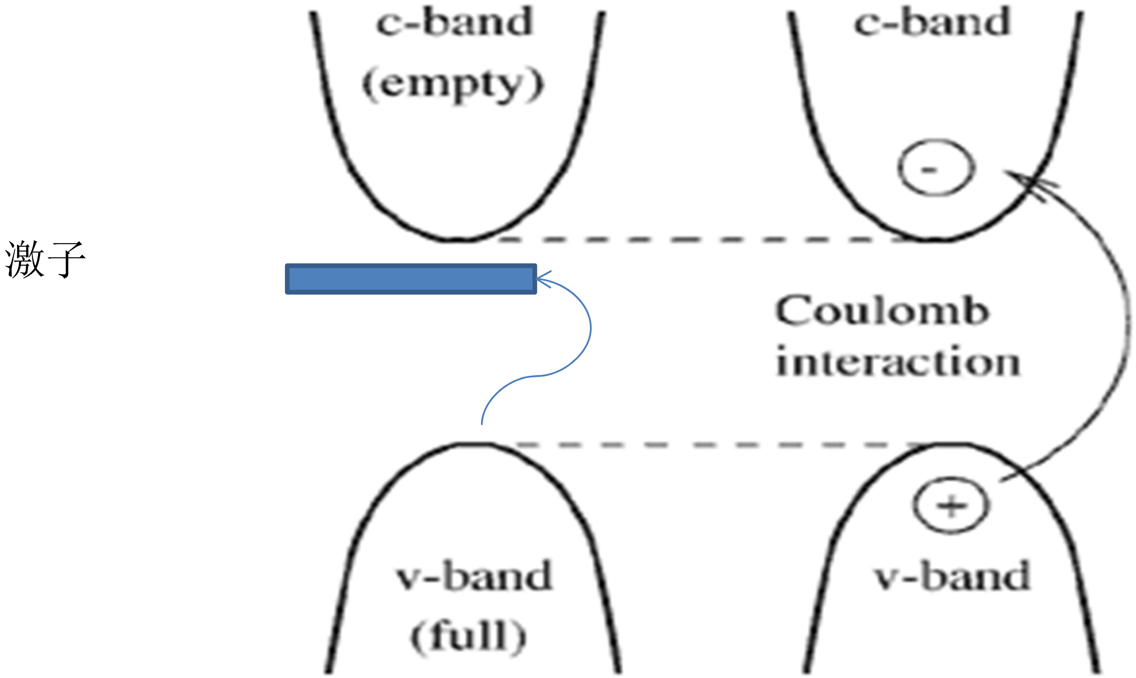

光吸收图解

低维系统 → 电子-空穴作用变强

→ 激子效应增强（激子能量更加低于导带底部）

光学吸收性质由激子决定！

11

多体效应

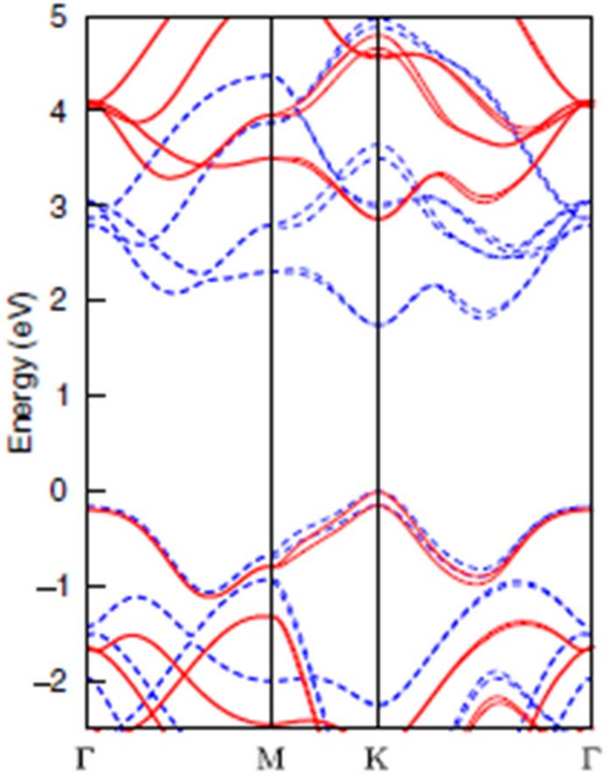

FIG. 1 (color online). Left: LDA (dashed blue curve) and *GW* (solid red curve) band structure of monolayer MoS_2. Top right:

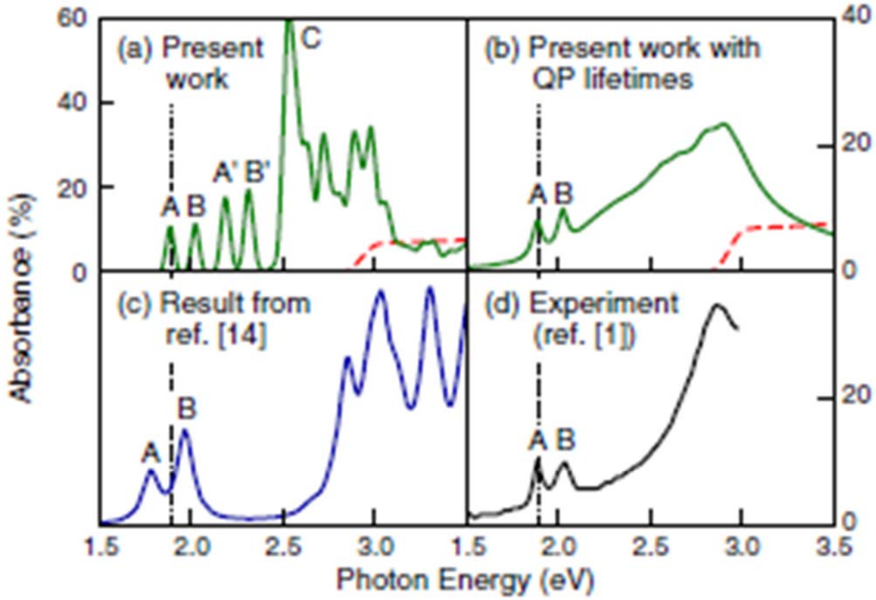

FIG. 2 (color online). (a) Absorption spectra of MoS_2 without (dashed red curve) and with (solid green curve) electron-hole interactions using a constant broadening of 20 meV. (b) Same calculated data as in Fig. 2(a), but using an *ab initio* broadening based on the electron-phonon interactions [27,28]. (c) Previous G_0W_0 calculation (in arbitrary units). Note that the region between 2.2 and 2.8 eV is completely flat. (d) Experimental absorbance [1].

多体效应

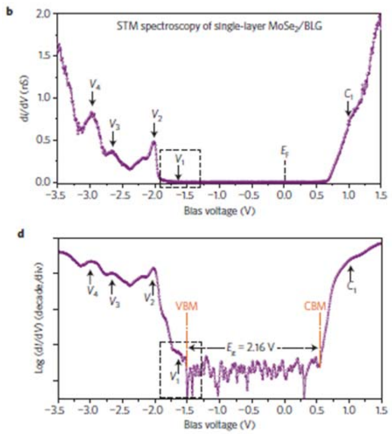

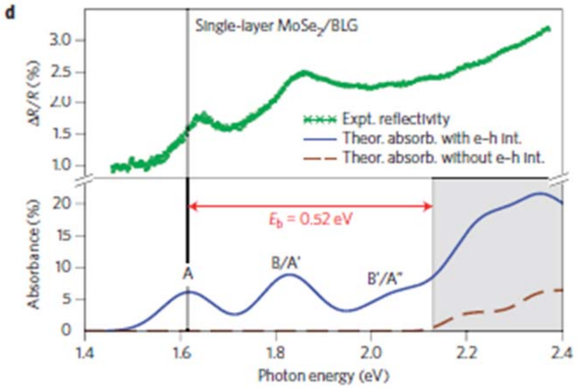

nature materials LETTERS
PUBLISHED ONLINE: 31 AUGUST 2014 | DOI: 10.1038/NMAT4061

Giant bandgap renormalization and excitonic effects in a monolayer transition metal dichalcogenide semiconductor

Miguel M. Ugeda, Aaron J. Bradley, Su-Fei Shi, Felipe H. da Jornada, Yi Zhang, Diana Y. Qiu, Wei Ruan, Sung-Kwan Mo, Zahid Hussain, Zhi-Xun Shen, Feng Wang, Steven G. Louie and Michael F. Crommie

问题:1 其他材料 MoS_2？WSe_2?激子效应。

2　　衬底的效应？

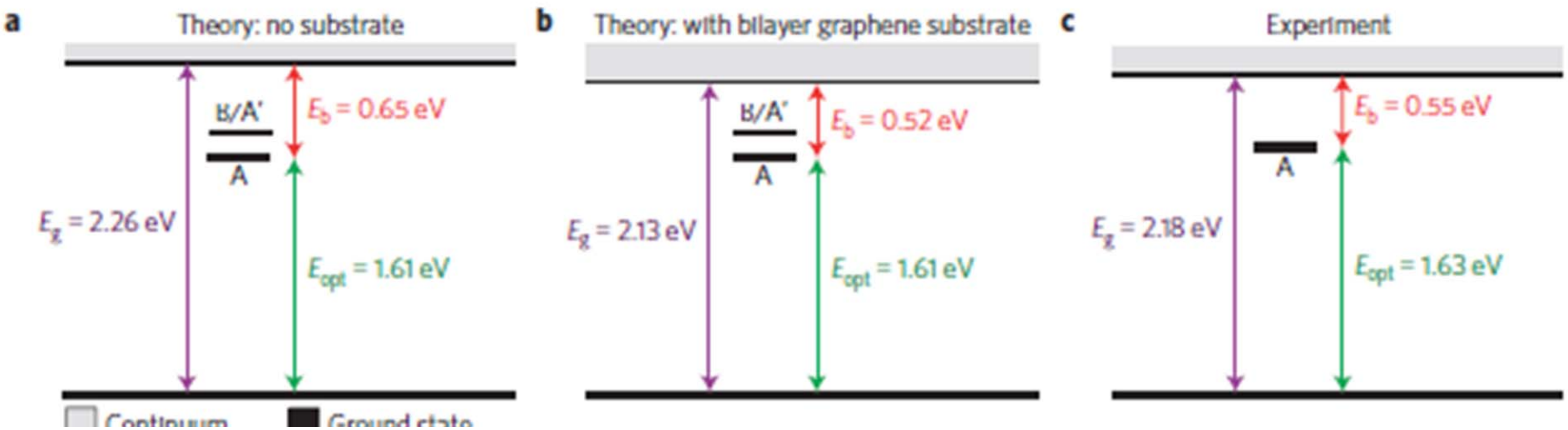

Valley index of Bloch electron

- Valley index of Bloch electron

  Degenerate energy extrema of Bloch bands in momentum space

  In atomically thin 2D crystals: graphene, BN, MoS_2 etc.

- Long lifetime of valley polarization expected

  Intervalley scattering suppressed by large k-space separation

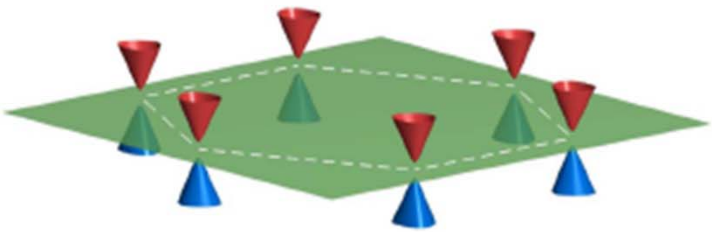

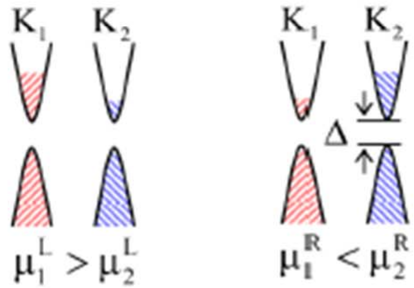

Valley polarization

Valley vs spin for information processing

Associated physical phenomena \ Index of Bloch electron	Spin	Valley	
Magnetic moment	✓	✓	Xiao, WY & Niu, PRL 07"
Hall effect	✓	✓	
Optical selection rule	✓	✓	WY, Xiao & Niu, PRB 08"

$\Omega(k) =$

- Valley physics from inversion symmetry breaking
- Valley can be manipulated in ways similar to spin
- Key quantities: Berry curvature & orbital magnetic moment

Hall effect

$$\Omega(k) = \nabla_k \times \langle u(k)|i\nabla_k|u(k)\rangle$$

Valley contrasting properties by ISB

Time-reversal symmetry	$\Omega(\boldsymbol{k}) = -\Omega(-\boldsymbol{k})$	$m(\boldsymbol{k}) = -m(-\boldsymbol{k})$
Space-inversion symmetry	$\Omega(\boldsymbol{k}) = \Omega(-\boldsymbol{k})$	$m(\boldsymbol{k}) = m(-\boldsymbol{k})$
Both symmetries	$\Omega(\boldsymbol{k}) = 0$	$m(\boldsymbol{k}) = 0$

- **Valley contrasting properties**
  - Opposite Ω & m for a time reversal pair of valleys
  - Necessary condition: inversion symmetry breaking (ISB)
- **Example: graphene with staggered sublattice potential**

∘ $\frac{\Delta}{2}$

• $-\frac{\Delta}{2}$

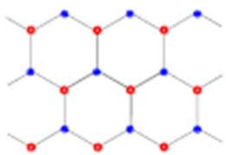

Massive Dirac fermion:

$$\hat{H} = at(\square k_x \hat{\sigma}_x + k_y \hat{\sigma}_y) + \frac{\Delta}{2}\hat{\sigma}_z$$

Valley contrasting Berry curvature

Berry curvature $\Omega(\boldsymbol{q}) = \tau_z \dfrac{3\Delta t^2}{2(\Delta^2 + 3q^2a^2t^2)^{3/2}}$ $\tau_z = 1\ (-1)$ at valley K (-K)

谷磁矩

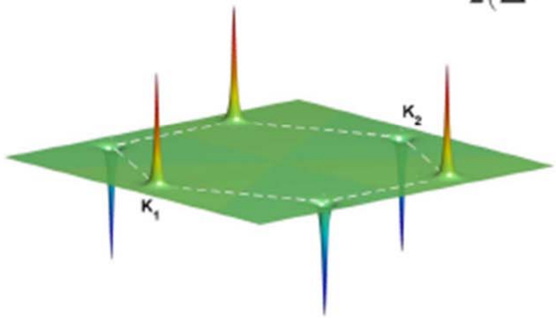

Valley Hall effect

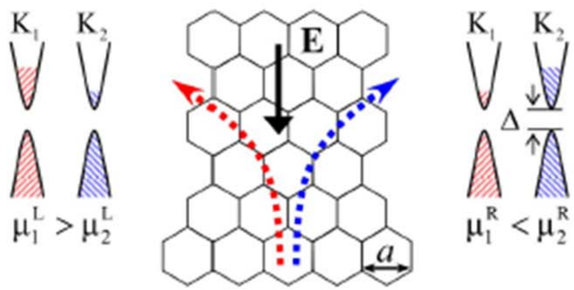

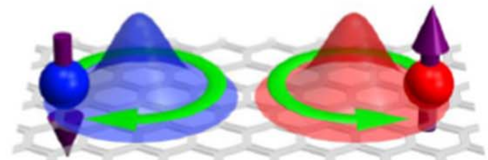

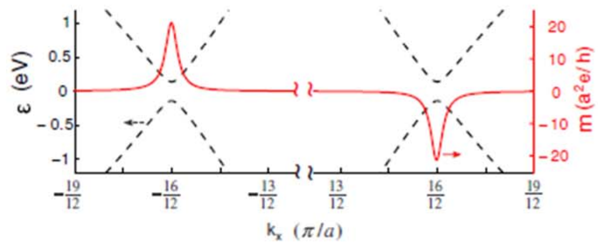

Gapped energy dispersion

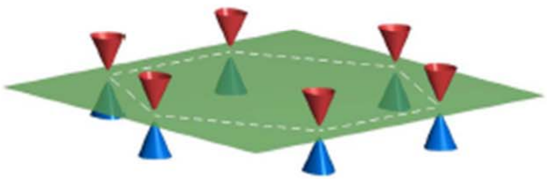

gapped Dirac cones

Xiao, WY & Niu, PRL 99, 236809 (2007)

Spin-valley coupled massive Dirac fermions

WX_2

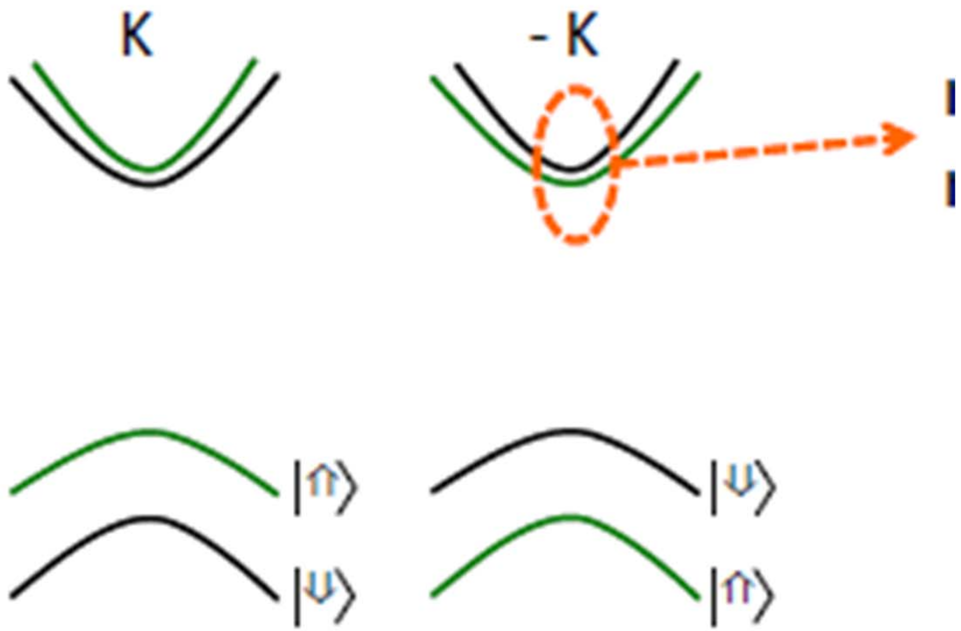

2 FET

摩尔定律：集成电路上可容纳的晶体管数目，约每隔18个月便会增加一倍。

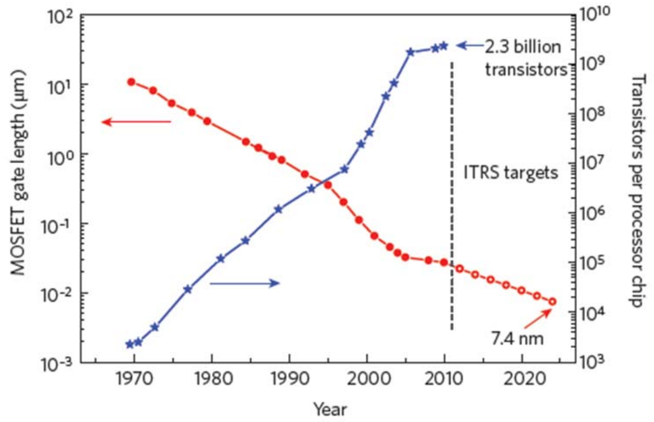

Figure 1 | Trends in digital electronics. Evolution of MOSFET gate length

挑战： 目前的计算机晶体管尺寸已经缩短到20 nm。下一个十年晶体管的沟道长度要小于10个纳米。**但块材硅做沟道的晶体管在10纳米以下的尺度由于显著的短沟道效应实际已经不能可靠工作了。**

可能的解决方案

1 可以改进硅的结构，

2 低维材料

- 1D nanotube
- 2D材料

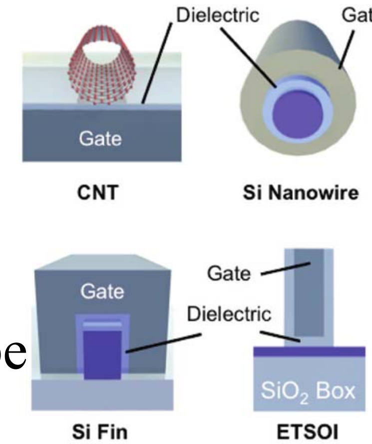

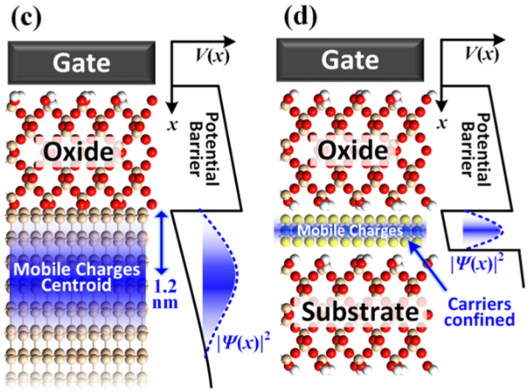

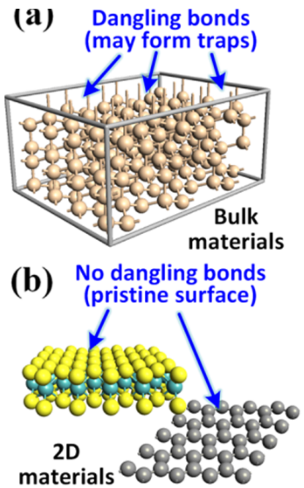

优势：门可控性好，削弱短沟道效应

无侧向的悬挂键，没有界面陷阱

nature nanotechnology LETTERS
PUBLISHED ONLINE: 30 JANUARY 2011 | DOI: 10.1038/NNANO.2010.279

Single-layer MoS_2 transistors

B. Radisavljevic[1], A. Radenovic[2], J. Brivio[1], V. Giacometti[1] and A. Kis[1]*

a

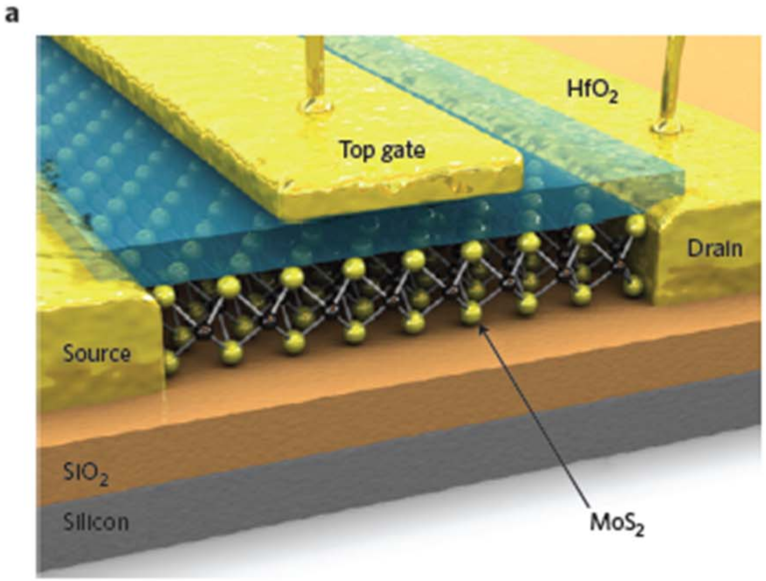

b

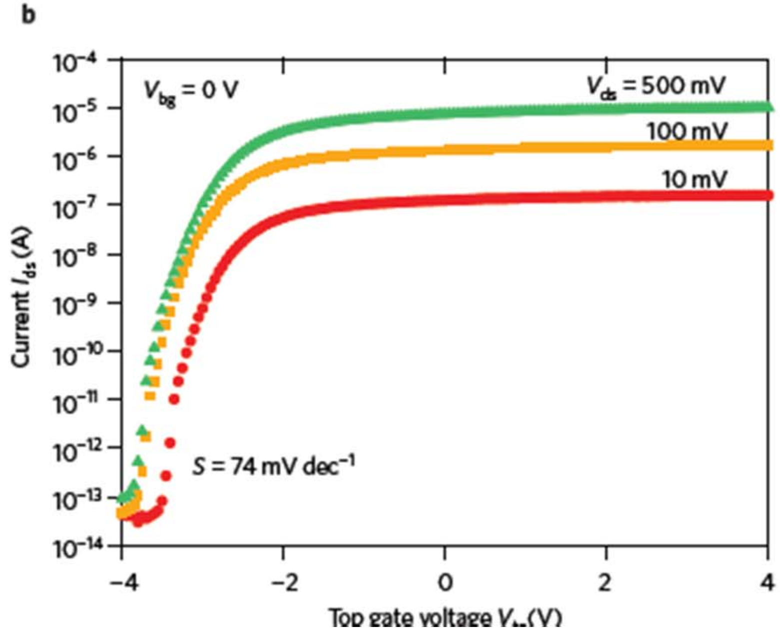

电子器件　光电器件　谷电子学　自旋电子学

载流子迁移率：
200 cm^2/V•s
沟道 L = 50 nm

问题：1 MoS_2-金属界面不是很清楚！
DFT肖特基势垒理论和实验对不上
Ti-单层: DFT欧姆 ⟺ 实验很大SBH

2 亚10nm FET能否很好工作？

Interfacial band structure

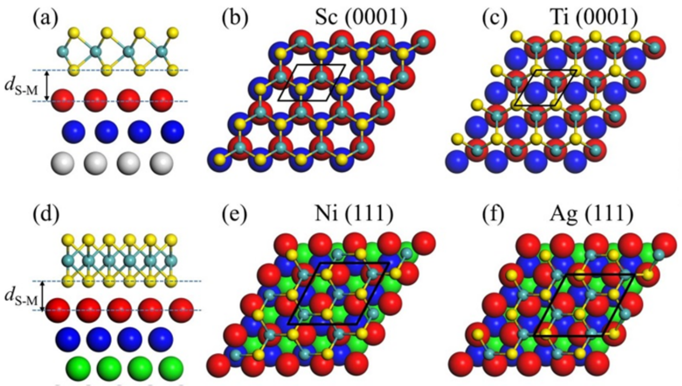

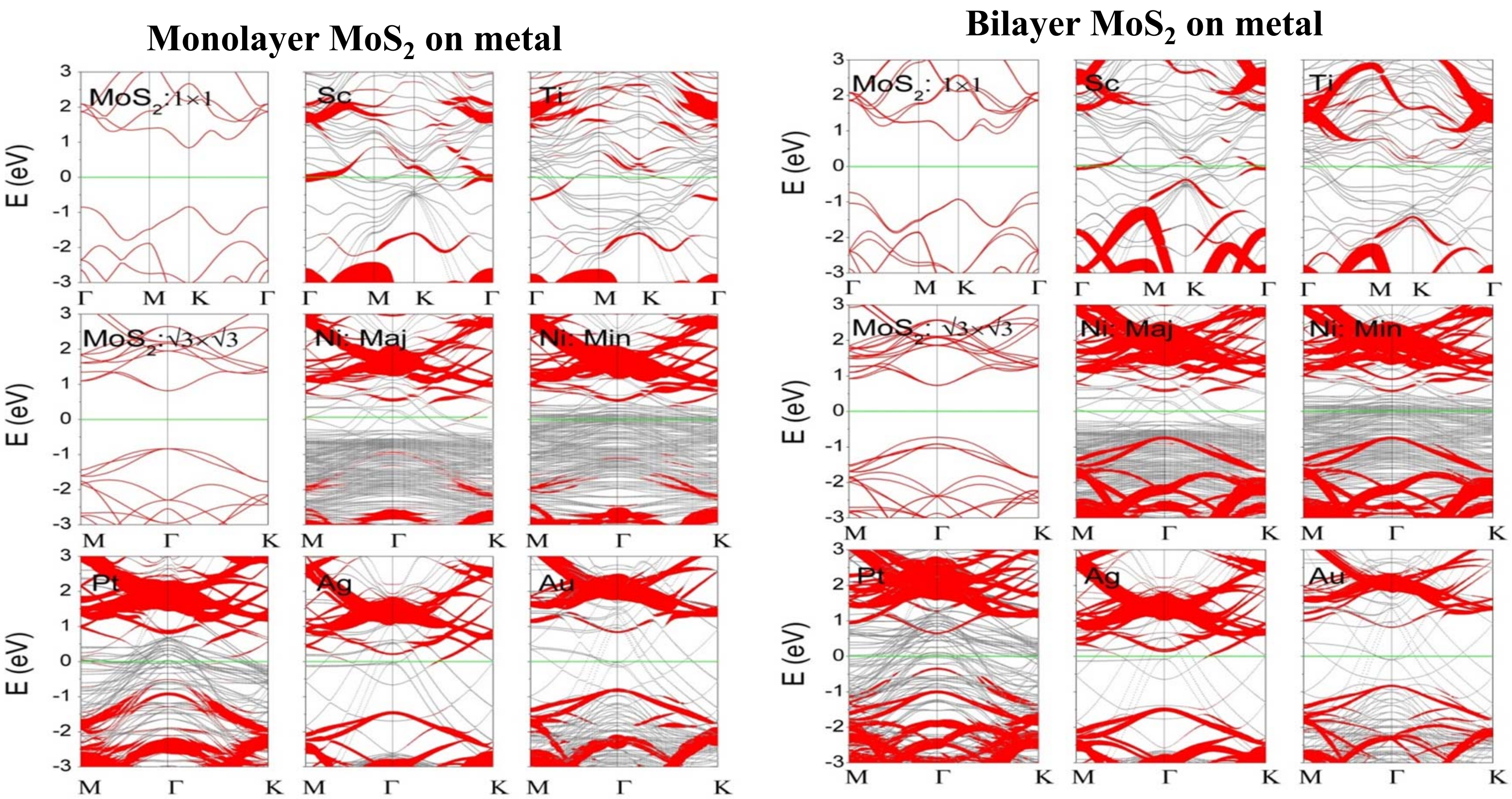

- The band structure of MoS_2 is identifiable clearly for MoS_2 on Au surface
- is slightly destroyed by Pt and Ag surfaces
- destroyed seriously by Sc, Ti, and Ni surfaces,
-

E$_f$

单层

双层

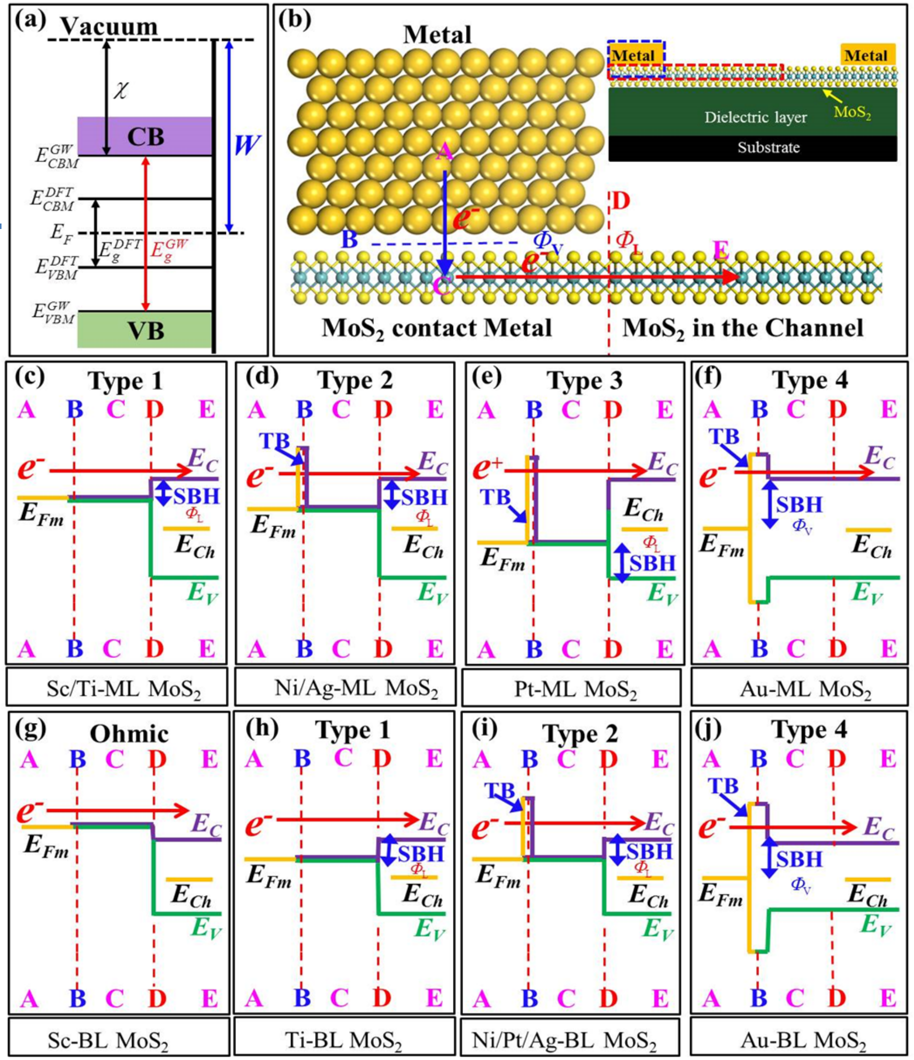

新方案

1. 区分两种界面 肖特基势垒

2. MoS_2的能隙1.8 (DFT) -2.8 eV （GW）能带做GW修正

理论

单层：大的 SBH NO Ohmic contact

双层：Sc Ohmic, Ti small SBH 71 meV

实验

单层： MoS_2-Ti: larger SBH

双层 MoS_2-Ti: with SBH ~65 meV at low temperature

(*Appl. Phys. Lett.* **2012,** *100*, 123104.)

这套计算肖特基势垒方案是普适的。

亚10nm MoS_2 FET

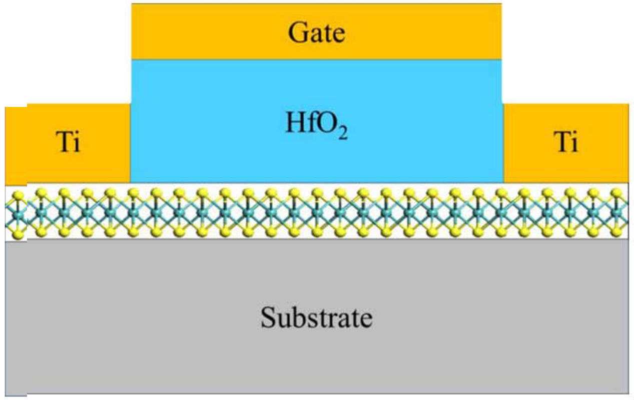

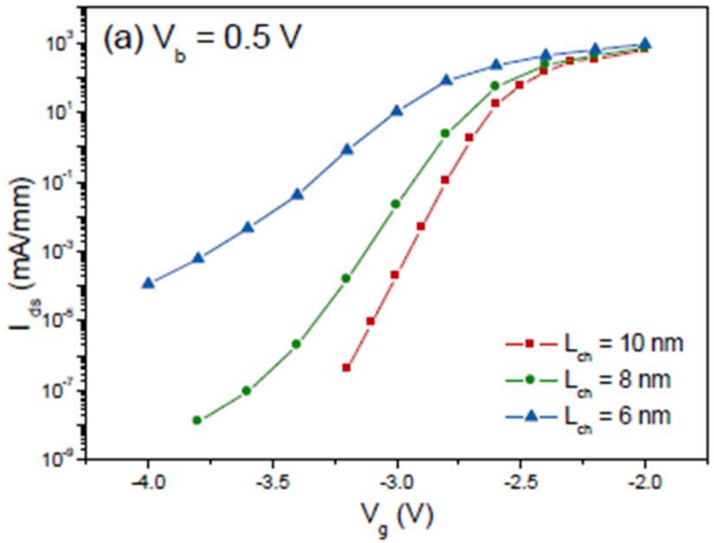

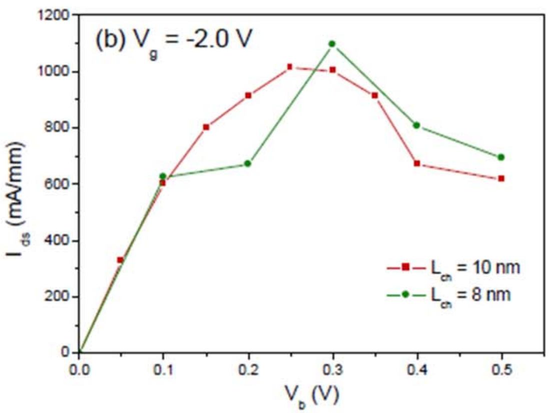

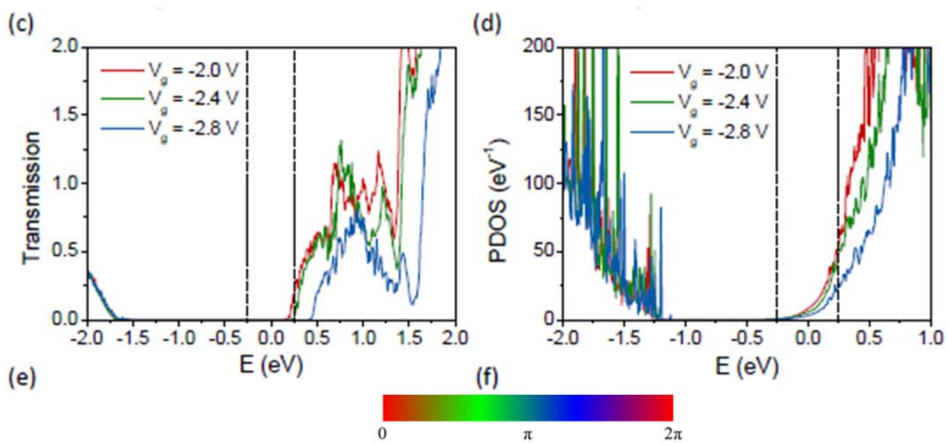

与其他FET对比 （相同的供应电压）

Category	L_{ch} (nm)	I_{on} (mA/mm)	I_{on}/I_{off}	*SS* (mV/dec)
MoS_2 FET	10	1030	1.0×10^4	62
CNT	9	630	1.0×10^4	94
Si nanowire	10	300	1.0×10^4	89
Si Fin	10	138	1.0×10^3	125
UTSOI	8	41	1.0×10^4	83

与国际半导体线路图（ITRS）2018年的要求对比

FET	L_{ch} (nm)	I_{on} (μA/μm)	I_{on}/I_{off}
MoS2 FET	10	2929	2.9×10^4
ITRS HP transistor 2018	10.2	1610	1.6×10^4

3 光电器件

LETTERS
nature nanotechnology
PUBLISHED ONLINE: 9 MARCH 2014 | DOI: 10.1038/NNANO.2014.26

Electrically tunable excitonic light-emitting diodes based on monolayer WSe_2 p–n junctions

Jason S. Ross[1], Philip Klement[2,3], Aaron M. Jones[3], Nirmal J. Ghimire[4,5], Jiaqiang Yan[5,6], D. G. Mandrus[4,5,6], Takashi Taniguchi[7], Kenji Watanabe[7], Kenji Kitamura[7], Wang Yao[8], David H. Cobden[2] and Xiaodong Xu[1,2]*

nature nanotechnology
LETTERS
PUBLISHED ONLINE: 9 MARCH 2014 | DOI: 10.1038/NNANO.2014.14

Solar-energy conversion and light emission in an atomic monolayer p–n diode

Andreas Pospischil, Marco M. Furchi and Thomas Mueller*

LETTERS
nature nanotechnology
PUBLISHED ONLINE: 9 MARCH 2014 | DOI: 10.1038/NNANO.2014.25

Optoelectronic devices based on electrically tunable p–n diodes in a monolayer dichalcogenide

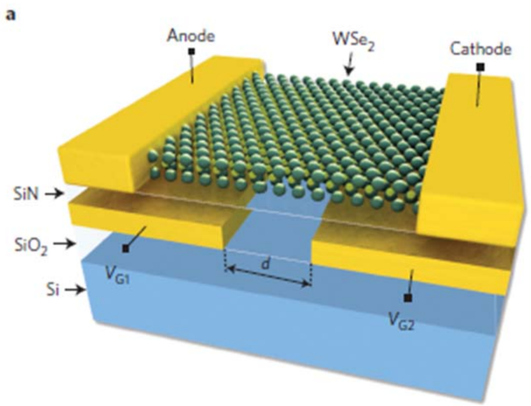

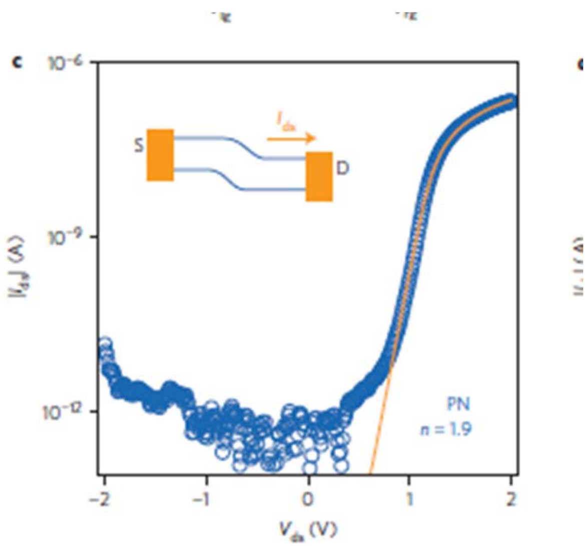

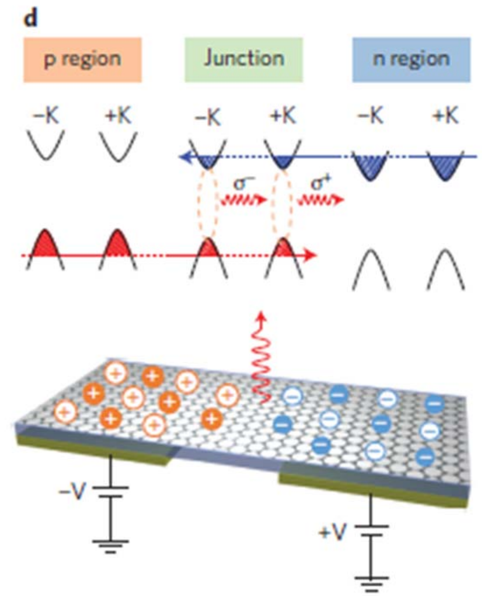

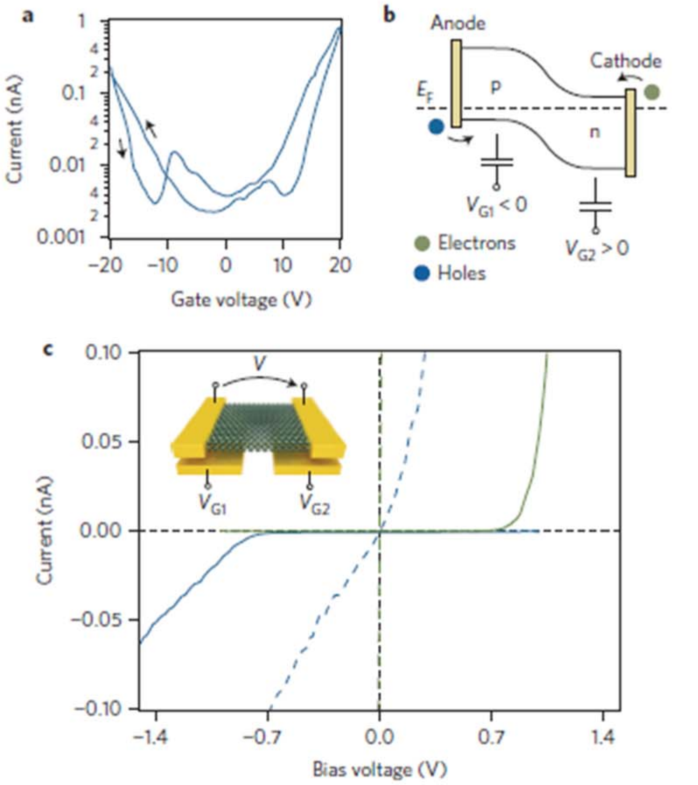

Figure 2 | Electrical characterization. a, Gate characteristic of the device (0.2 V bias voltage). Both electrons ($V_{G1} = V_{G2} > 10$ V) and holes ($V_{G1} = V_{G2} < -10$ V) can be injected into the channel. The curve was obtained by scanning the gate voltage from −20 V to 20 V and back. **b**, Band diagram when operating as a p–n junction diode. Asymmetric contact metallization allows more efficient electron (green) and hole (blue) injection. **c**, *I–V* characteristics of the device in the dark for biasing conditions as shown in the inset: p–n (solid green line; $V_{G1} = -40$ V, $V_{G2} = 40$ V), n–p (solid blue line; $V_{G1} = 40$ V, $V_{G2} = -40$ V), n–n (dashed green line; $V_{G1} = V_{G2} = 40$ V), p–p (dashed blue line; $V_{G1} = V_{G2} = -40$ V).

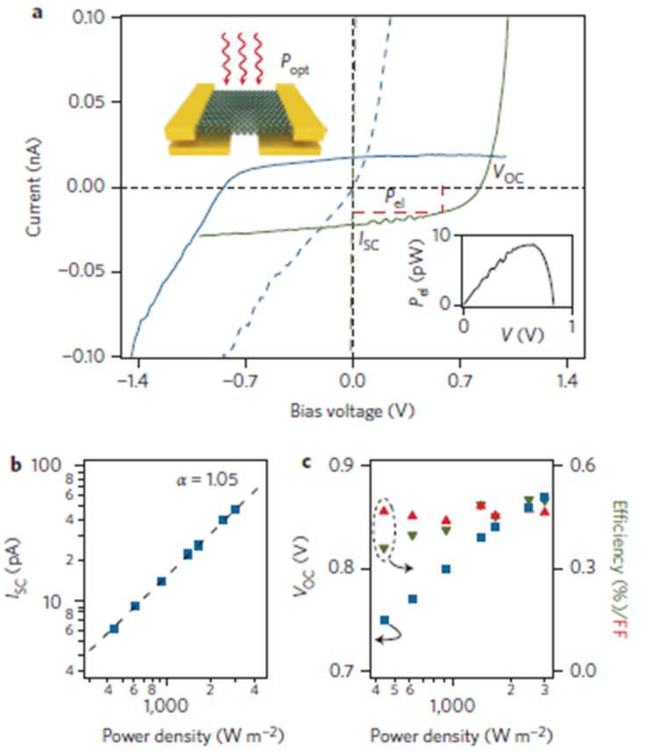

Figure 3 | Device operation as solar cell and photodiode. a, *I–V* characteristics of the device under optical illumination with 1,400 W m^{-2}. The biasing conditions are the same as in Fig. 2c: p–n (solid green line; $V_{G1} = -40$ V, $V_{G2} = 40$ V), n–p (solid blue line; $V_{G1} = 40$ V, $V_{G2} = -40$ V), n–n (dashed green line; $V_{G1} = V_{G2} = 40$ V), p–p (dashed blue line; $V_{G1} = V_{G2} = -40$ V). When operated as a diode (solid lines), electrical power (P_{el}) can be extracted. Top inset: Schematic of experiment. Lower inset: P_{el} versus voltage under incident illumination of 1,400 W m^{-2}. Maximum power conversion efficiency is obtained for $V = 0.64$ V and $I = 14$ pA. The red dashed rectangle in the main panel shows the corresponding power area. **b**, Short-circuit current I_{SC}. Symbols, measurements; dashed line, fit of power law. **c**, Open-circuit voltage V_{OC} (blue symbols), fill factor FF (red symbols) and power conversion efficiency η_{PV} (green symbols). All parameters are plotted versus incident light intensity.

LETTERS NATURE NANOTECHNOLOGY DOI: 10.1038/NNANO.2014.150

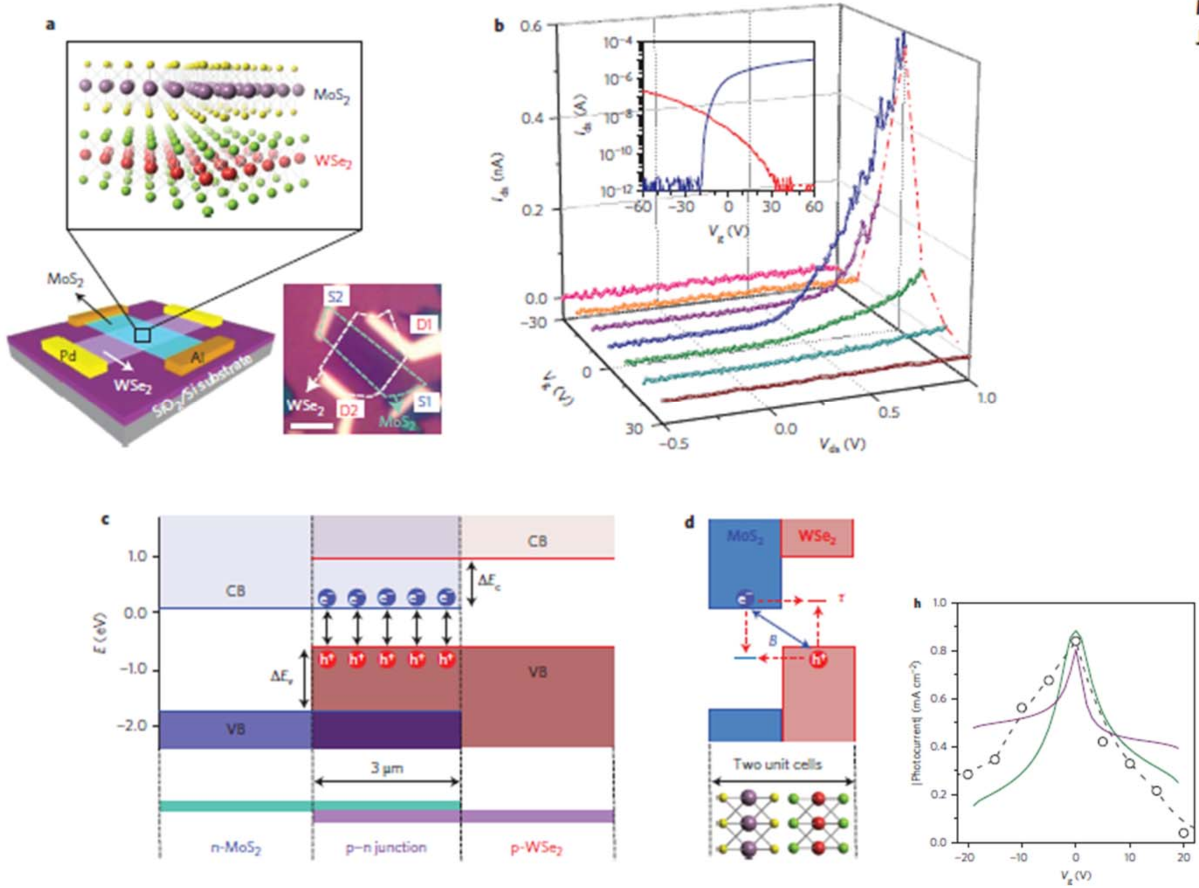

Atomically thin p–n junctions with van der Waals heterointerfaces

Chul-Ho Lee[1,2,3], Gwan-Hyoung Lee[4], Arend M. van der Zande[5], Wenchao Chen[6], Yilei Li[1], Minyong Han[7], Xu Cui[8], Ghidewon Arefe[8], Colin Nuckolls[2], Tony F. Heinz[1,9], Jing Guo[6], James Hone[8] and Philip Kim[1]*

问题: 1 同质MX2 不用门 能否实现p-n 结？

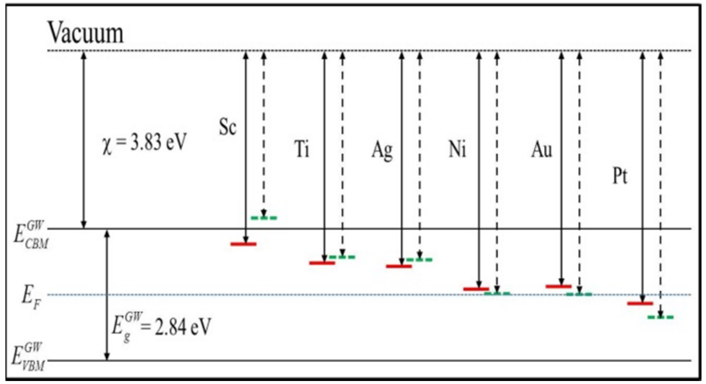

Pt

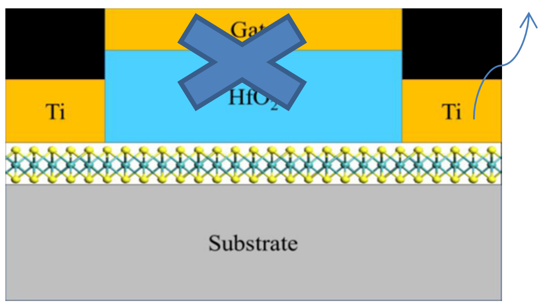

2. 实现TFET（隧穿场效应管）？

4 谷电子学自旋电子学器件

Spin dependent optical selection rule

Valley optical selection rule

Valley & spin optical selection rule

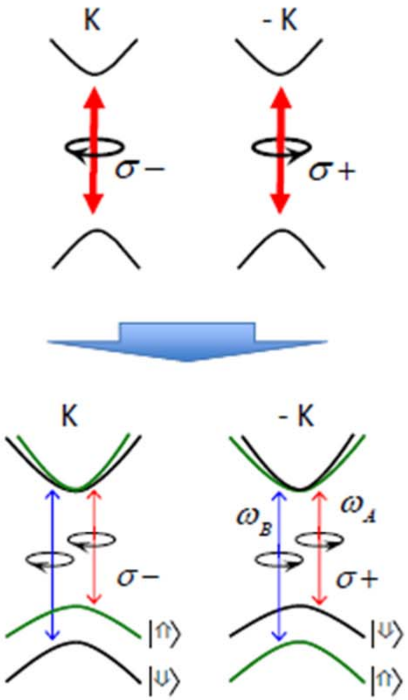

WY, Xiao & Niu, PRB 77, 235406 (2008)

Xiao, Liu, Feng, Xu & WY, PRL 108, 196802 (2012)

Selective excitation of valley & spin controlled by light polarization & freq

光学选择性的起源

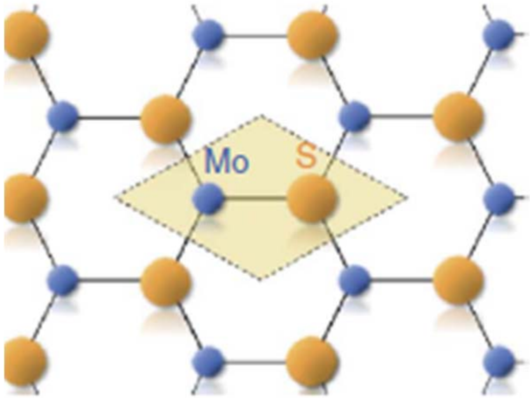

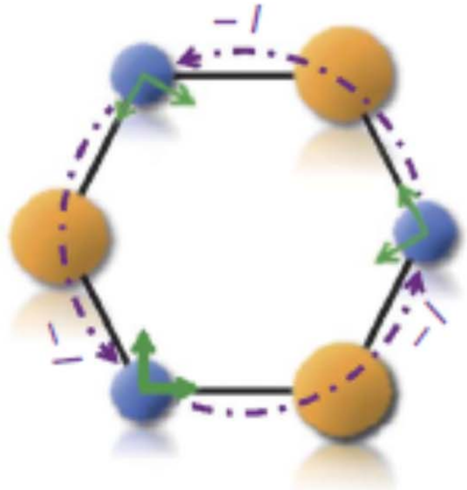

$$w_l(\mathbf{r}) = e^{il\varphi} f(\theta, r),$$

$$\hat{C}_3 \,|\, v(\mathbf{K}_\pm)\rangle = |\, v(\mathbf{K}_\pm)\rangle,$$

$$\hat{C}_3 \,|\, c(\mathbf{K}_\pm)\rangle = e^{\mp i 2\pi/3} \,|\, c(\mathbf{K}_\pm)\rangle,$$

$$|\phi_c\rangle = |d_{z^2}\rangle, \qquad |\phi_v^\tau\rangle = \frac{1}{\sqrt{2}}(|d_{x^2-y^2}\rangle + i\tau|d_{xy}\rangle),$$

Now the chiral optical selectivity of the valleys can be deduced. The bottom of the conduction bands at the valleys, dominated by the $l=0$ d-states on Mo, bears an overall azimuthal quantum number $m_\pm = \pm 1$, at $\mathbf{K}_\pm$. At the top of the valence bands, $m_\pm = 0$. Then for an optical transition at $\mathbf{K}_\pm$, the angular momentum selection rule indicates that $\Delta m_\pm = \pm 1$, corresponding to the absorption of left- and right-handed photons. Therefore, our den-

MoS_2 的在整个布里渊区的旋光选择性　以及实验的观测

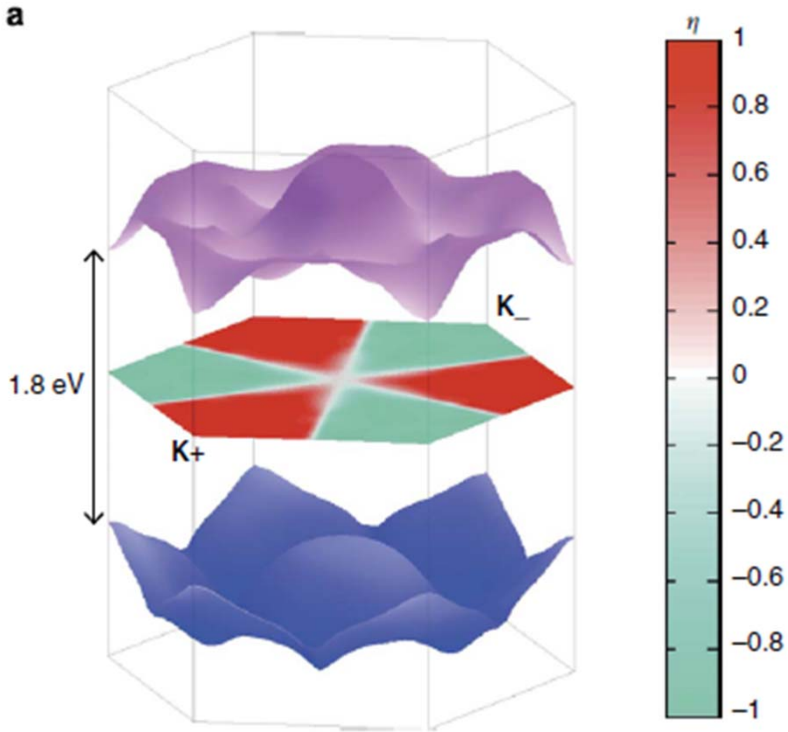

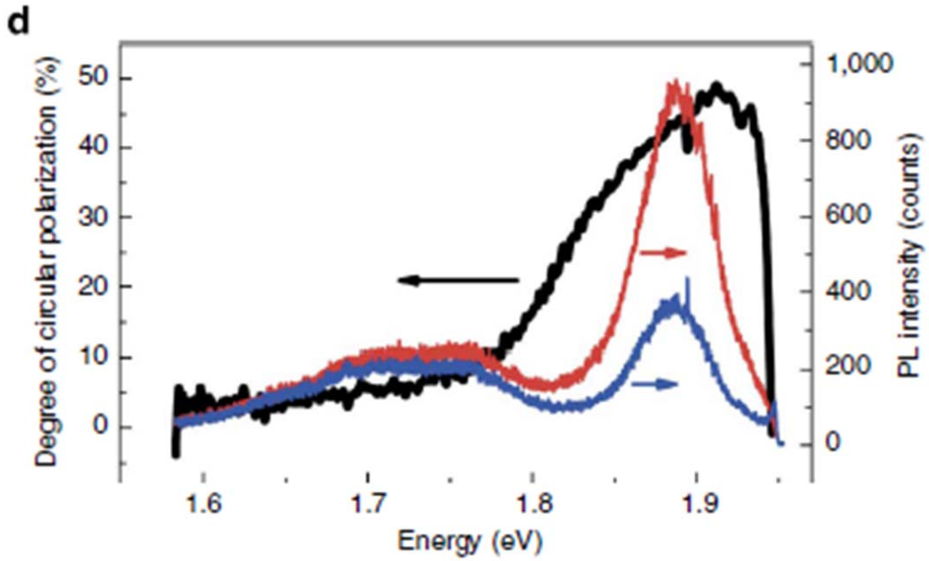

门压对发光谱的控制

LETTERS
PUBLISHED ONLINE: 11 AUGUST 2013 | DOI: 10.1038/NNANO.2013.151
nature nanotechnology

Optical generation of excitonic valley coherence in monolayer WSe_2

Aaron M. Jones[1], Hongyi Yu[2], Nirmal J. Ghimire[3,4], Sanfeng Wu[1], Grant Aivazian[1], Jason S. Ross[5], Bo Zhao[1], Jiaqiang Yan[4,6], David G. Mandrus[3,4,6], Di Xiao[7], Wang Yao[2]* and Xiaodong Xu[1,5]*

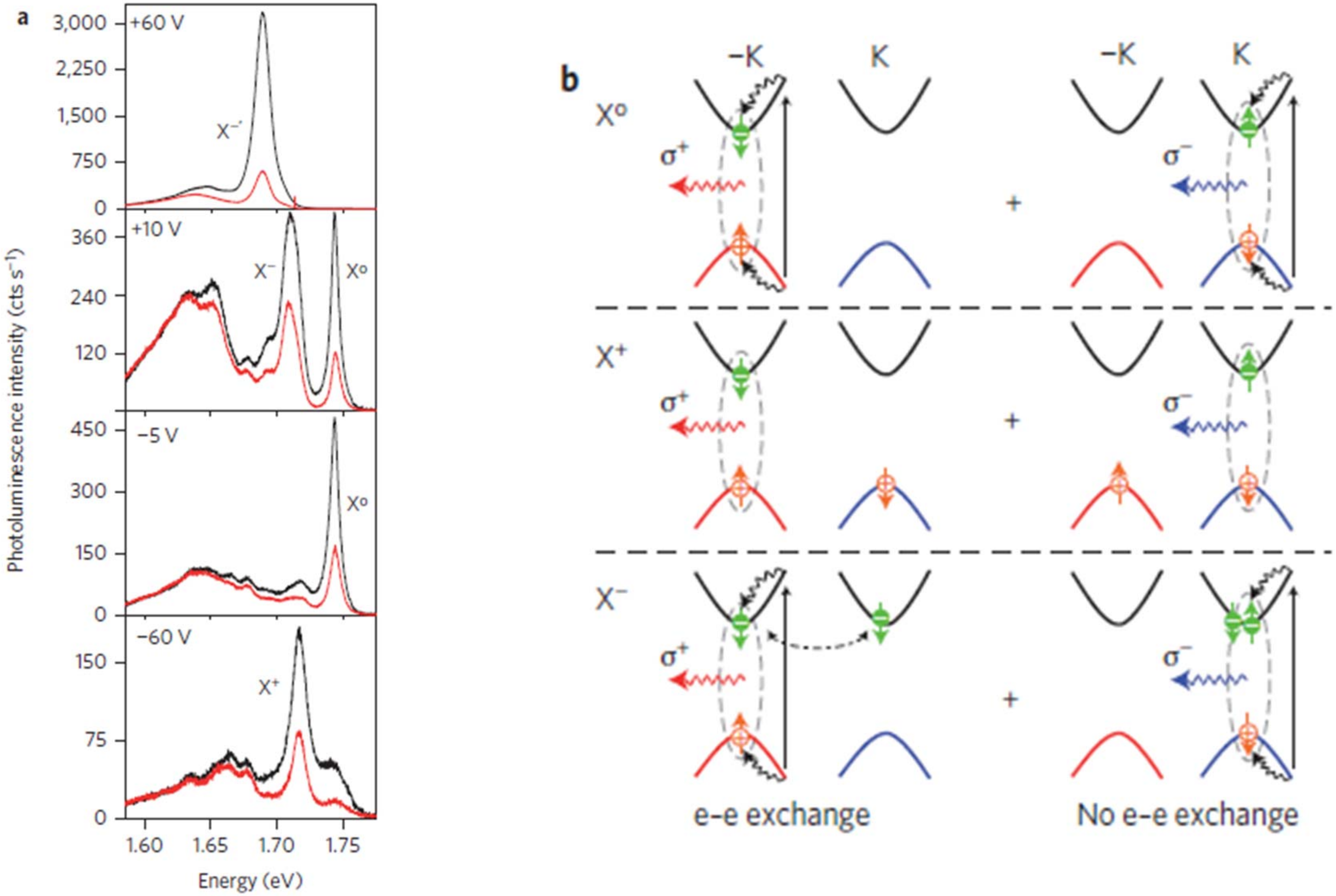

Electrically Switchable Chiral Light-Emitting Transistor
Y. J. Zhang *et al.*
Science **344**, 725 (2014);
DOI: 10.1126/science.1251329

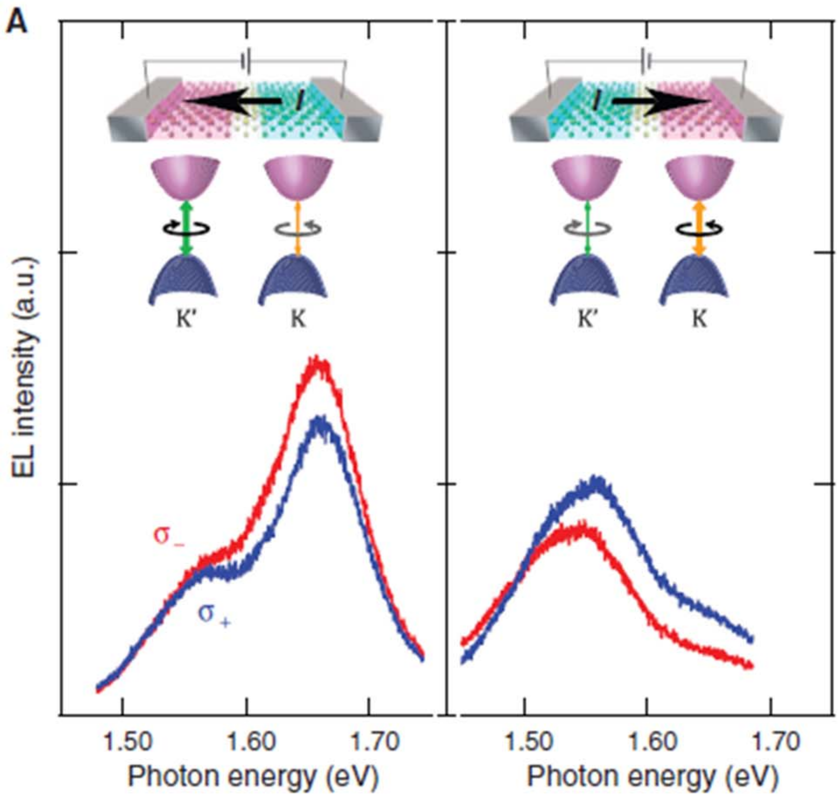

偏压方向改变， 旋光性也改变

双层MoS2 的谷极化

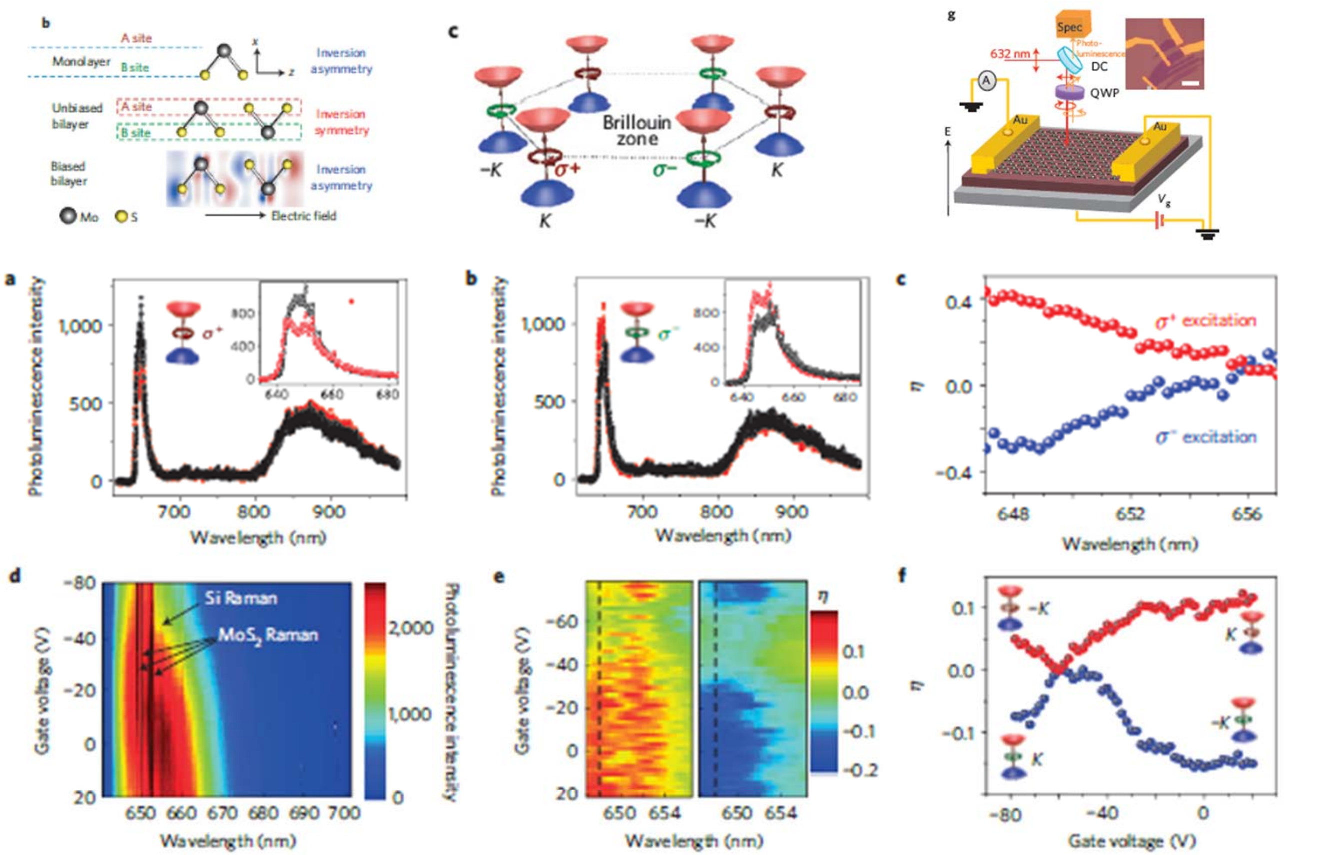

Figure 2 | Electrical control of valley magnetic moment in bilayer MoS_2 FETs. a,b, Polarization-resolved photoluminescence excited by σ^+ (a) and σ^- (b) light at $V_g = 0$. Insets: zoomed-in photoluminescence spectra around 650 nm. Black (red): $P(\sigma^+)$ ($P(\sigma^-)$) signals. c, Degree of photoluminescence polarization as a function of wavelength. Red (blue): σ^+ (σ^-) excitation. d, Photoluminescence intensity map as a function of wavelength and gate voltage. e, Degree of photoluminescence polarization as a function of wavelength and gate voltage. The left (right) plot is obtained for σ^+ (σ^-) excitation. f, Degree of photoluminescence polarization as a function of gate voltage at 648 nm (line cuts along the dashed lines in e). Red (blue) dots denote σ^+ (σ^-) excitation.

nature physics LETTERS
PUBLISHED ONLINE: 27 JANUARY 2013 | DOI: 10.1038/NPHYS2524

Electrical tuning of valley magnetic moment through symmetry control in bilayer MoS_2

Sanfeng Wu[1], Jason S. Ross[2], Gui-Bin Liu[3], Grant Aivazian[1], Aaron Jones[1], Zaiyao Fei[1], Wenguang Zhu[4,5,6], Di Xiao[5,7], Wang Yao[3], David Cobden[1] and Xiaodong Xu[1,2]*

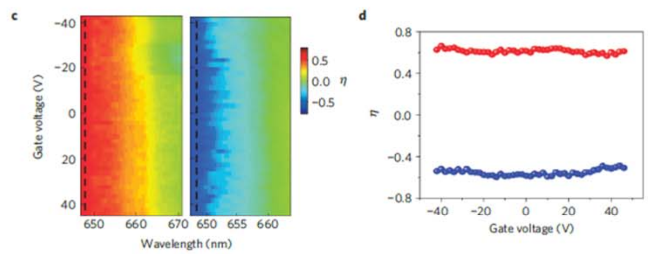

单层

$$\mathbf{m}_s(k) = (\hat{z}\mu_B/2m_e)\sum_{n\neq s}(|P_+^{ns}(k)|^2 - P_-^{ns}(k)|^2)/(\varepsilon_n(k) - \varepsilon_s(k)),$$

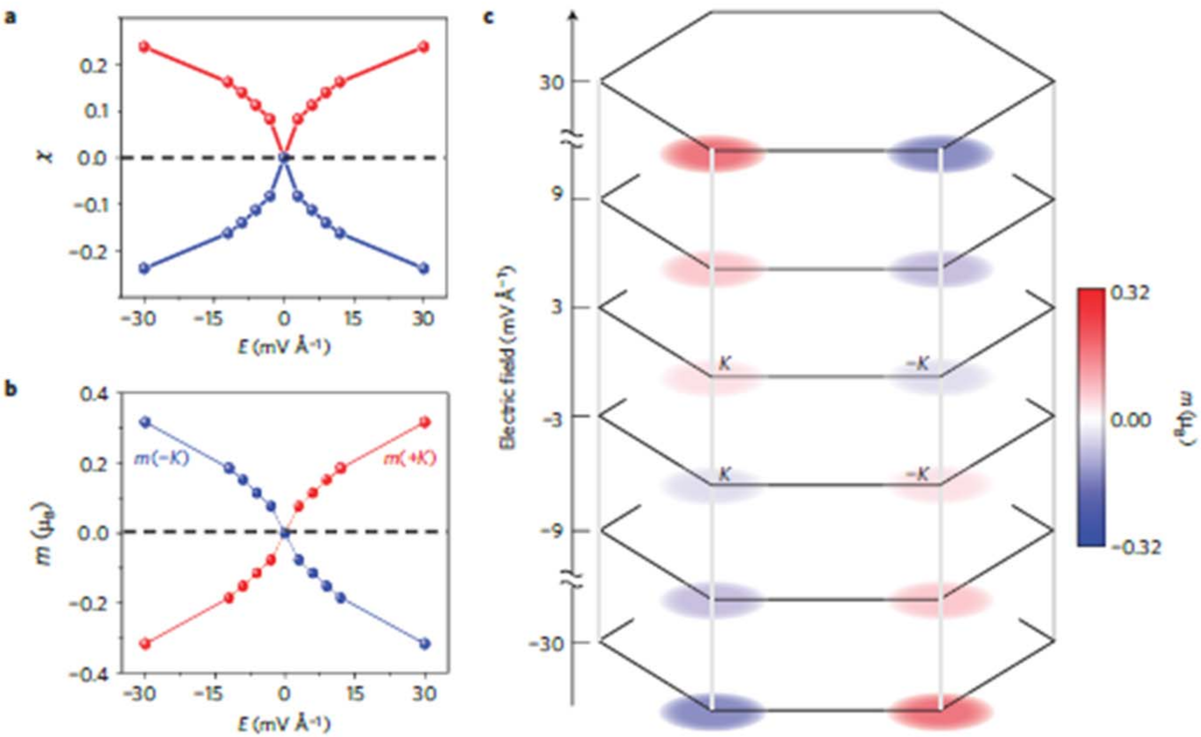

Figure 4 | DFT calculation of magnetoelectric effect and associated circular dichroism. a, Absorption circular dichroism χ as a function of electric field. The positive (negative) value represents σ^+ (σ^-) excitation. **b**, **m** at ±K as a function of electric field, which shows that **m** is an odd function of electric field. **c**, Colour map of **m** as a function of electric fields near ±K points in the momentum space.

双层加电场 引起自旋劈裂

nature physics ARTICLES
PUBLISHED ONLINE: 28 JULY 2013 | DOI: 10.1038/NPHYS2691

Zeeman-type spin splitting controlled by an electric field

Hongtao Yuan[1,2]*, Mohammad Saeed Bahramy[1,3]*, Kazuhiro Morimoto[1], Sanfeng Wu[4], Kentaro Nomura[3,5], Bohm-Jung Yang[3], Hidekazu Shimotani[1,6], Ryuji Suzuki[1], Minglin Toh[7], Christian Kloc[7], Xiaodong Xu[4,8], Ryotaro Arita[1,3], Naoto Nagaosa[1,3] and Yoshihiro Iwasa[1,3]*

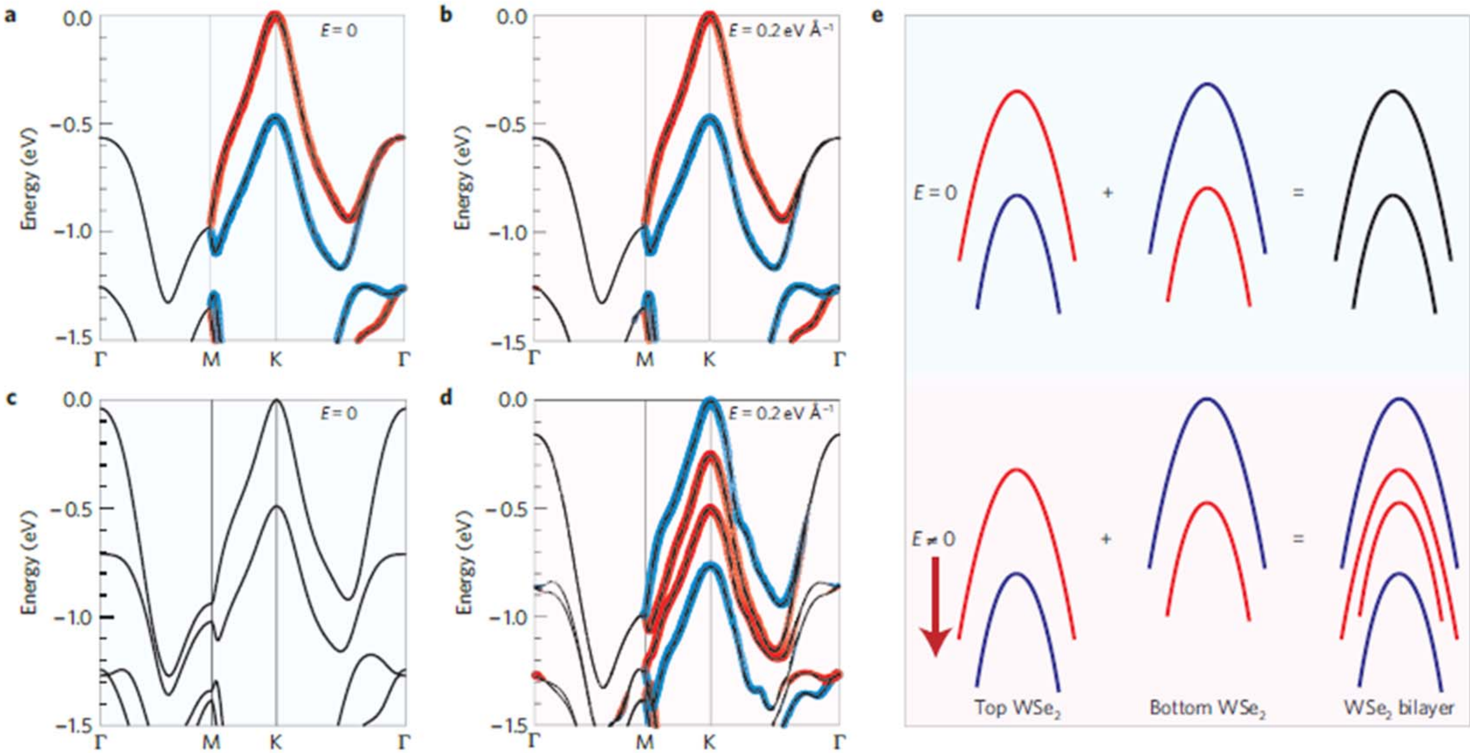

Figure 5 | Origin of out-of-plane spin polarization in WSe_2 under the external electric field. a,b, Electronic band structures of a monolayer of WSe_2 under

旋光伏特效应（CPGE)

nature nanotechnology
ARTICLES
PUBLISHED ONLINE: 7 SEPTEMBER 2014 | DOI: 10.1038/NNANO.2014.183

Generation and electric control of spin–valley-coupled circular photogalvanic current in WSe_2

Hongtao Yuan[1,2], Xinqiang Wang[3,4], Biao Lian[1], Haijun Zhang[1], Xianfa Fang[3,4], Bo Shen[3,4], Gang Xu[1], Yong Xu[1], Shou-Cheng Zhang[1,2], Harold Y. Hwang[1,2]* and Yi Cui[1,2]*

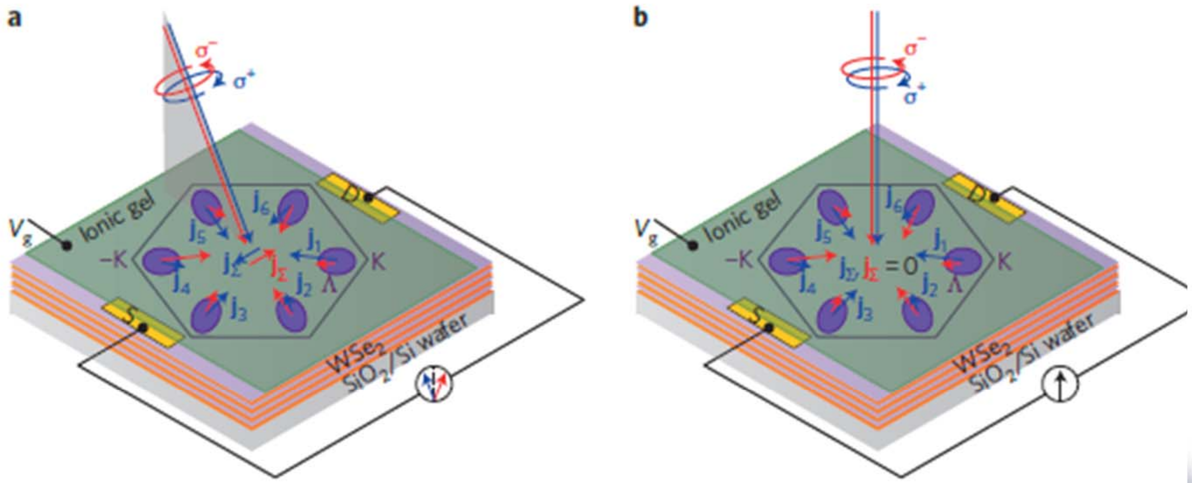

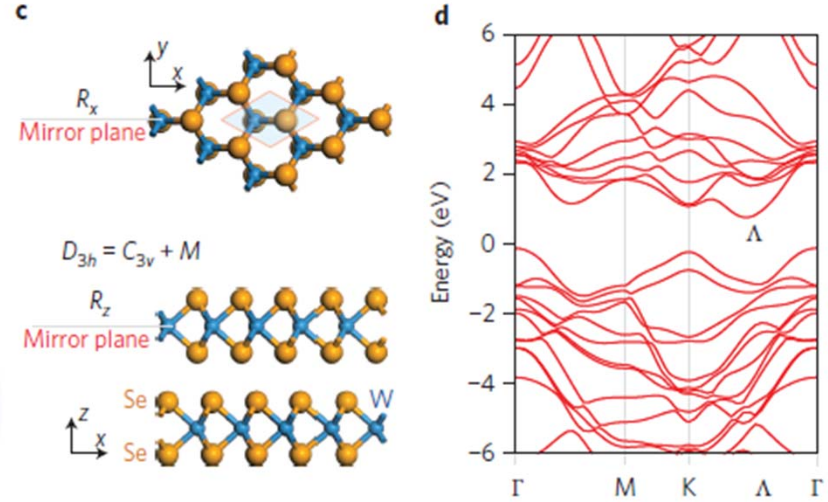

Figure 1 | Field-effect transistor on a WSe_2 surface with a transparent ionic gel gate. **a**, Distribution of electron fluxes in valleys induced by circularly polarized light at oblique incidence. The total helicity-dependent electric current arises in the direction perpendicular to the light incidence plane. **b**, Distribution of electron fluxes in valleys for normally incident circularly polarized light. Ellipsoids show electron valleys in the Brillouin zone, represented by the hexagonal shape. Points K and −K are shown. S, source; D, drain; V_g, gate voltage. Left-handed (σ^-; red) or right-handed (σ^+; blue) circularly polarized light induces different currents (**J** vectors) in the electron valleys. The total current in **a** is shown by the red and blue arrows labelled $\mathbf{J}_\Sigma$.

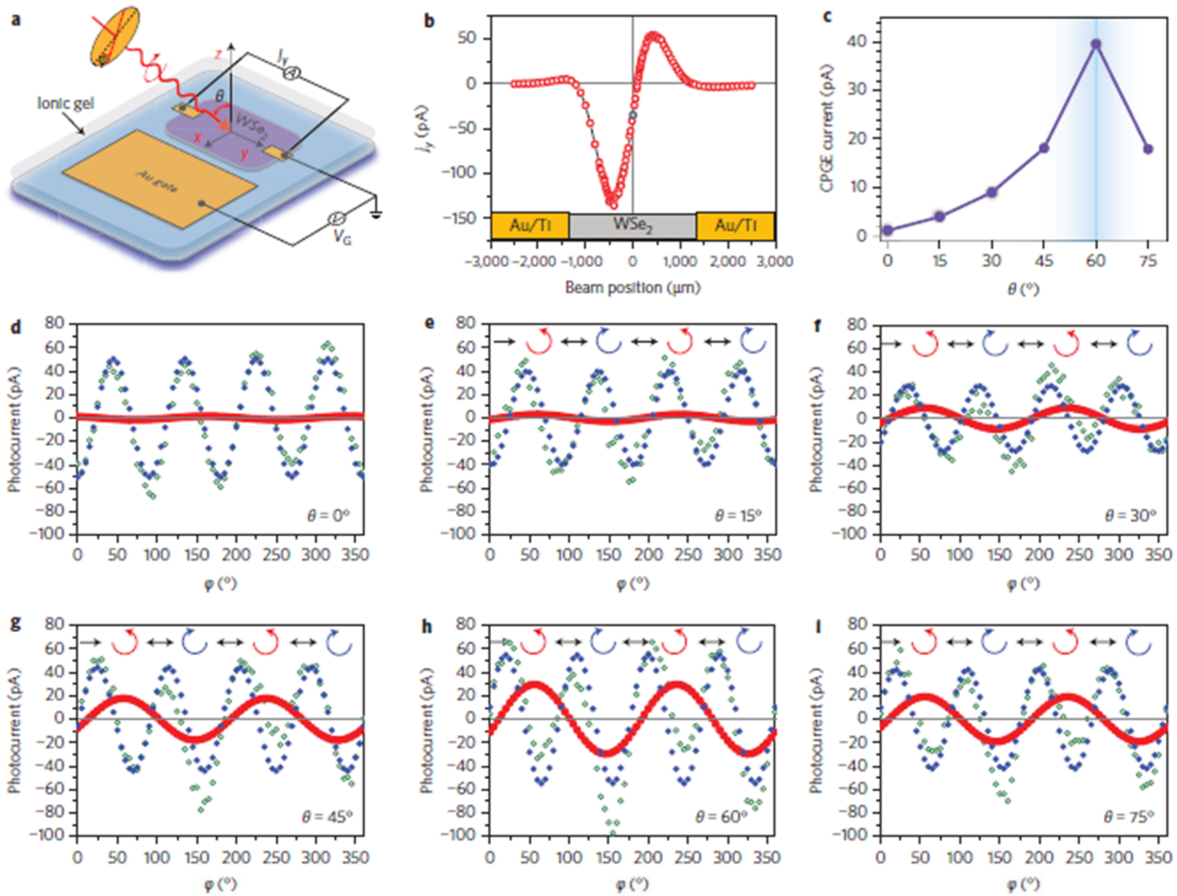

Figure 2 | Schematic diagram and incident angle-dependent CPGE measurement of ambipolar WSe_2 EDLTs. a, Schematic structure of a typical WSe_2 EDLT with ionic gel gating. By applying a gate voltage V_G to the lateral Au gate electrode, ions in the gel are driven to the WSe_2 surface, forming a perpendicular electric field at the EDL interface. Even without an external bias, a relatively low carrier-density accumulation layer exists at the WSe_2 surface owing to the Fermi level realignment between the gel/WSe_2 interface. **b**, A position-dependent photocurrent from sweeping the laser spot across the two electrodes (yellow rectangles shown at the bottom) in the zero-biased WSe_2 EDLT device with a fixed polarization. **c**, CPGE photocurrent j_{CPGE} as a function of the incident angle, θ, which shows a peak around $\theta = 60°$ (indicated by the blue line). **d–i**, Light polarization dependence of photocurrent j_y in a biased WSe_2 EDLT, measured at $y = 0$ with different incident angles θ. The open green circles are the measured j_y following the form $j_y = C\sin 2\varphi + L\sin 4\varphi + A$. The filled blue circles are the photocurrent that originates from the linear photogalvanic effect and obtained from the $\pi/2$-period oscillation term $L\sin 4\varphi$ by fitting. The filled red dots are the CPGE photocurrent with a π-periodic current oscillation. Polarization of the incident light at each quarter-wave plate angle, φ, is given by the symbols shown in the inset of each figure.

$$j_y = C\sin 2\varphi + L\sin 4\varphi + A$$

$L\sin 4\varphi$ corresponding to the linear photogalvanic effect (LPGE).

$$j_{CPGE} = \eta\gamma I \sin\theta \sin 2\varphi,$$

$$j_{CPGE} = C\sin 2\varphi$$

谷霍尔效应　自旋霍尔效应

$\sigma^{\rm int} = (e^2/\hbar) \int [d\boldsymbol{k}] f(\boldsymbol{k}) \Omega($

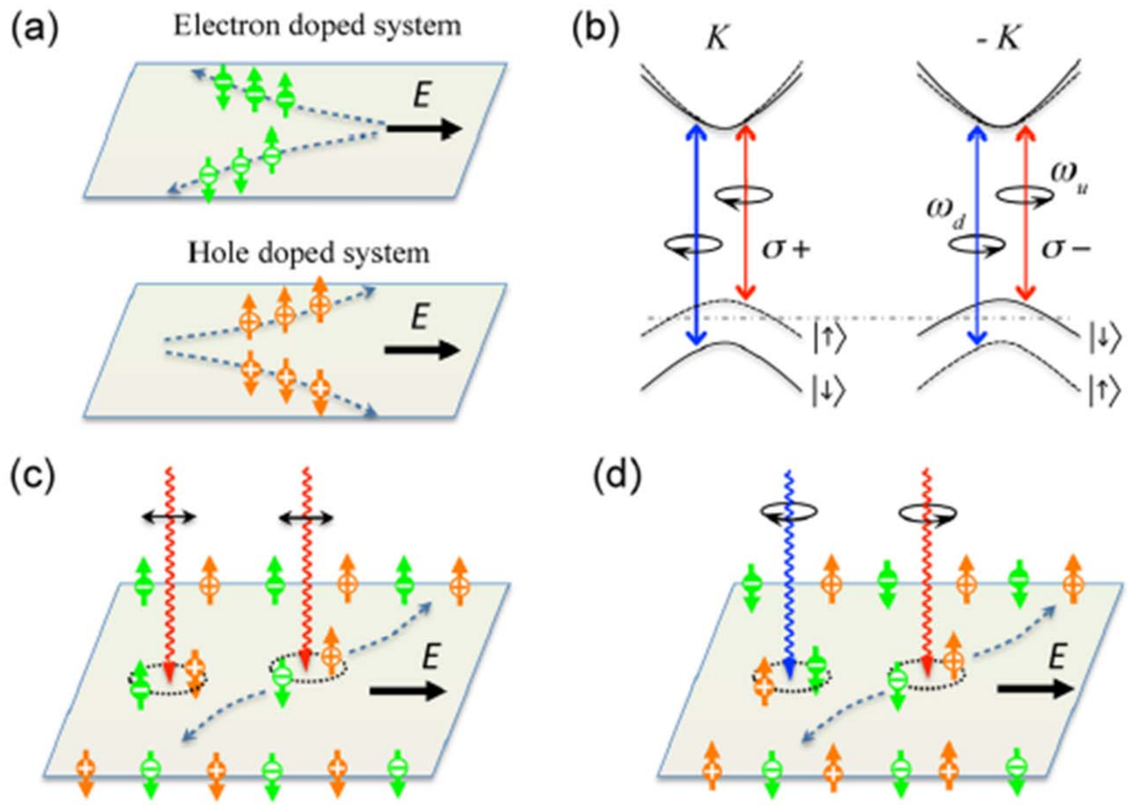

FIG. 2 (color online). Coupled spin and valley physics in monolayer group-VI dichalcogenides. The electrons and holes

The valley Hall effect in MoS_2 transistors
K. F. Mak *et al.*
Science **344**, 1489 (2014);
DOI: 10.1126/science.1250140

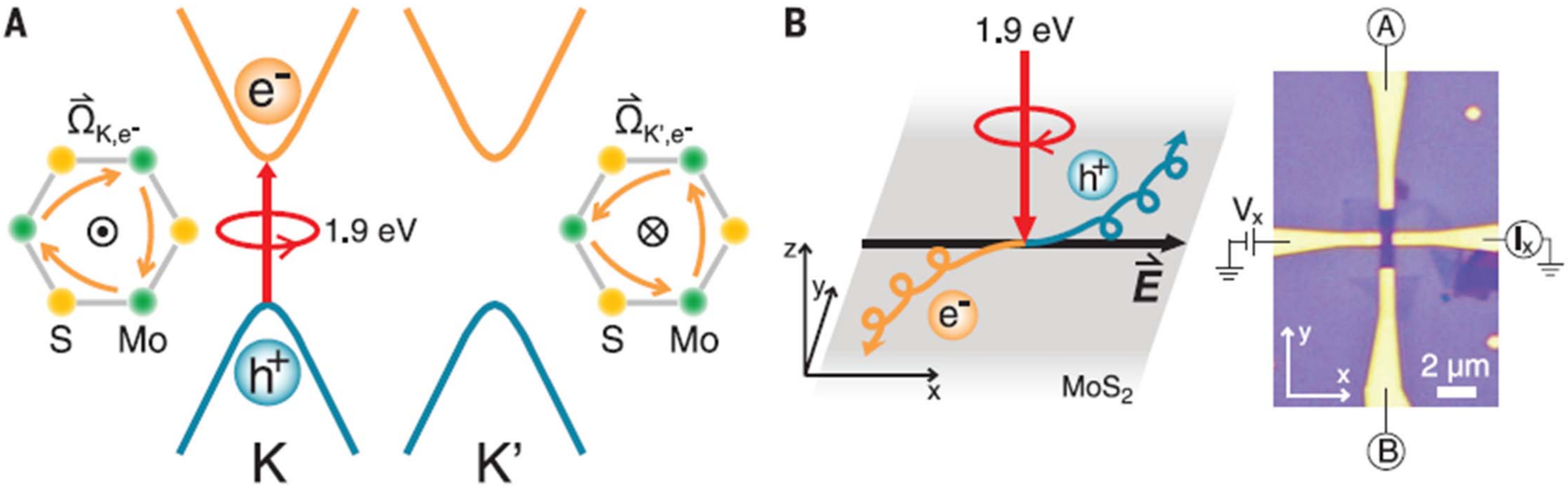

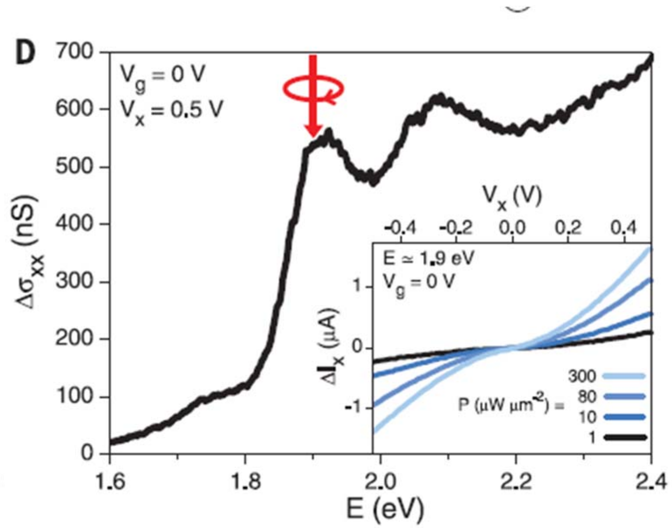

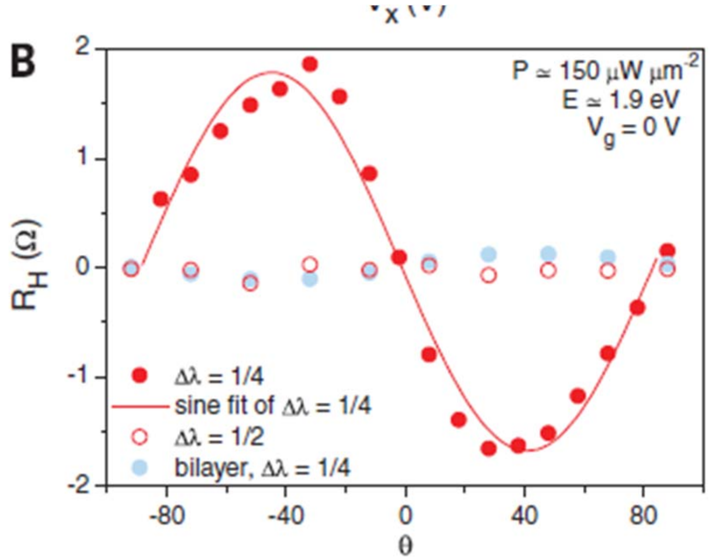

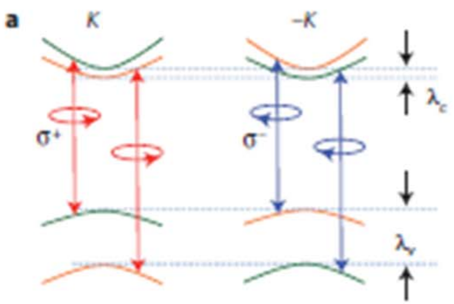

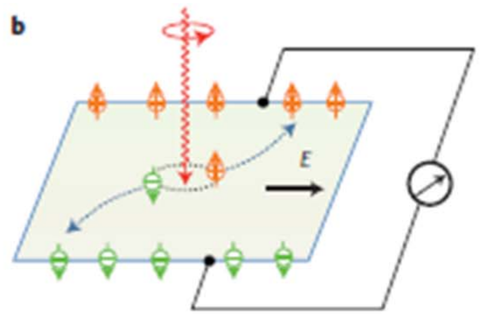

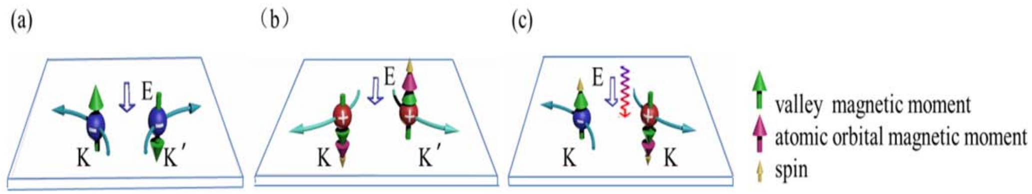

问题: 1　证明是自旋流

2 双层WS_2加垂直电场 也应该观察谷霍尔效应

3 谷轨道磁矩霍尔效应？

Title: Magnetic Control of Valley Pseudospin in Monolayer WSe_2

Authors: G. Aivazian[1], Zhirui Gong[2], Aaron M. Jones[1], Rui-Lin Chu[3], J. Yan[4,5], D. G. Mandrus[4,5,6], Chuanwei Zhang[3], David Cobden[1], Wang Yao[2*], X. Xu[1,7*]

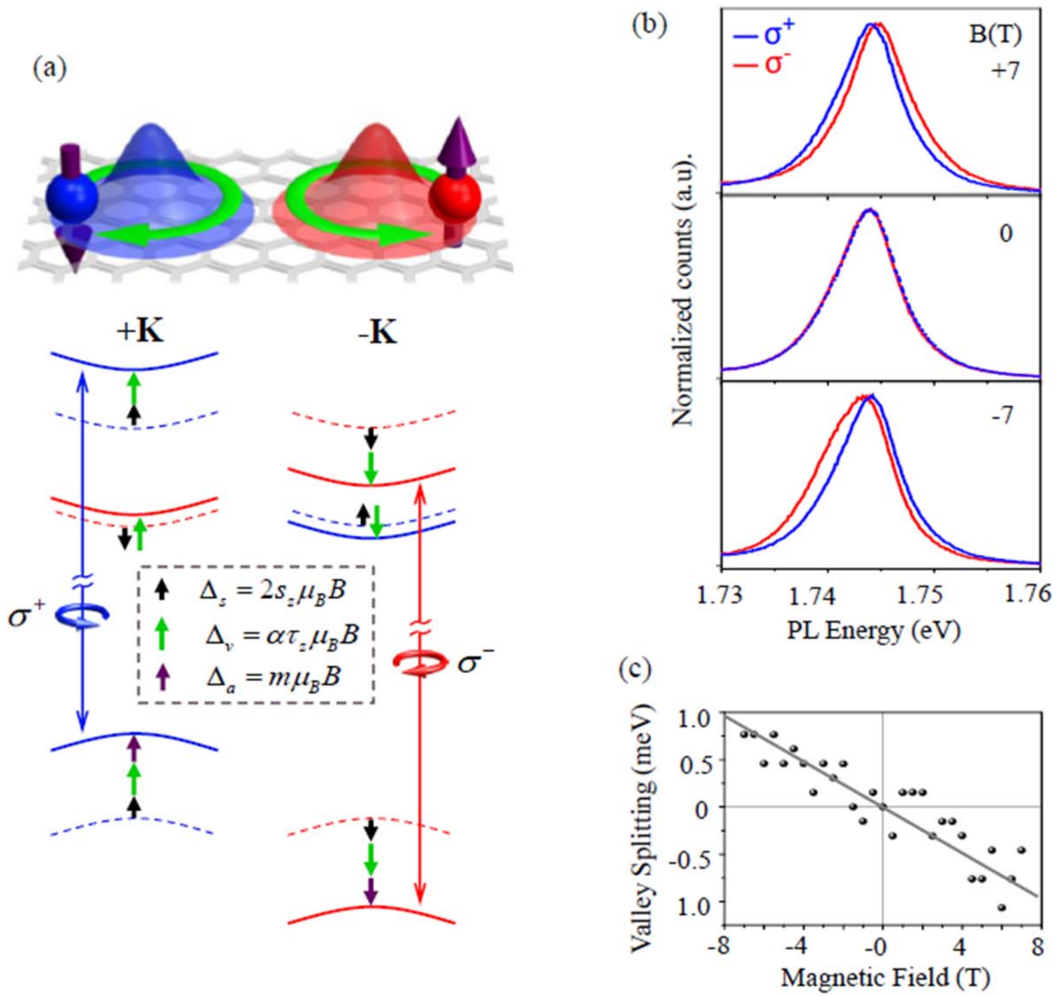

5 其他2D 材料 硅烯

Silicene on metals

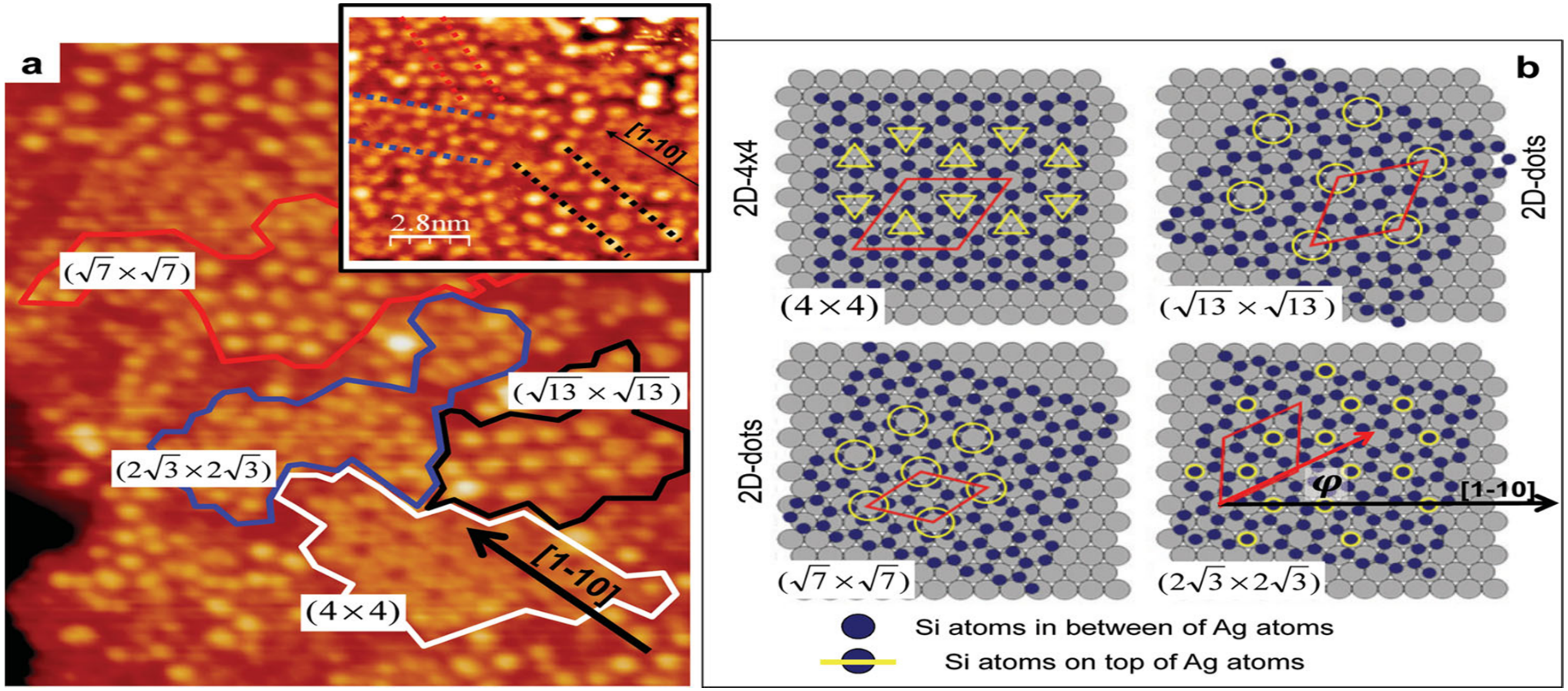

Ag index

(a) STM characterization of multi-oriented silicene domains on Ag(111)
(b) Sequence of ball models

Adv. Mater. **24**, 5088-5093 (2012)
Phys. Rev. Lett. **108**, 155501 (2012)
Phys. Rev. Lett. **107**, 076802 (2011)

Absence of Dirac cone: (3×3) silicene on (4×4) Ag phase

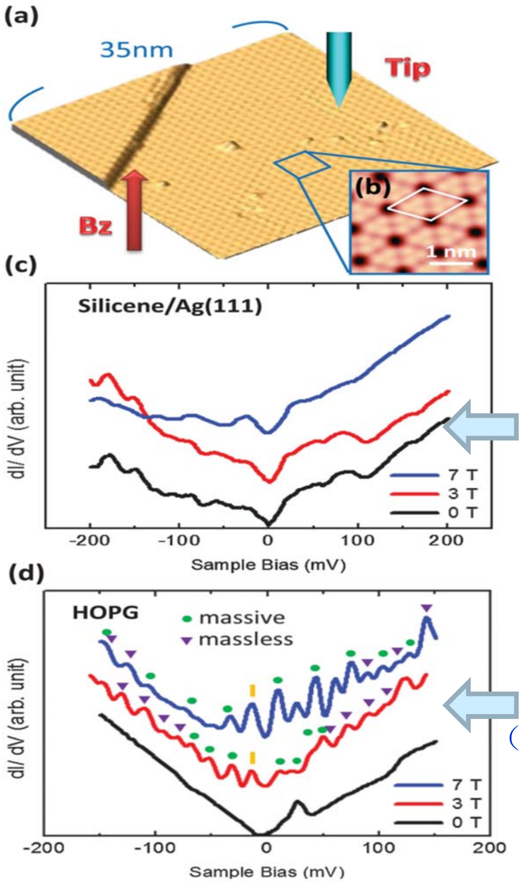

scanning tunneling spectra (STS)

No Landau levels (LLs)

LLs appear in the HOPG
(Highly Ordered Pyrolytic Graphite)

PRL 110, 076801 (2013)

No Ag substrate

With Ag substrate

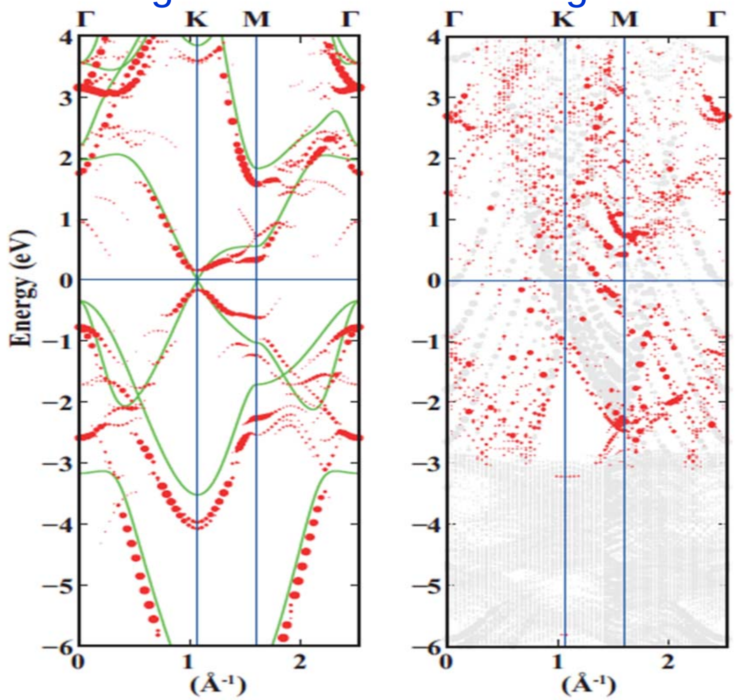

Red color: Si orbitals

PRB 88, 035432 (2013)

Absence of Dirac cone: other phases

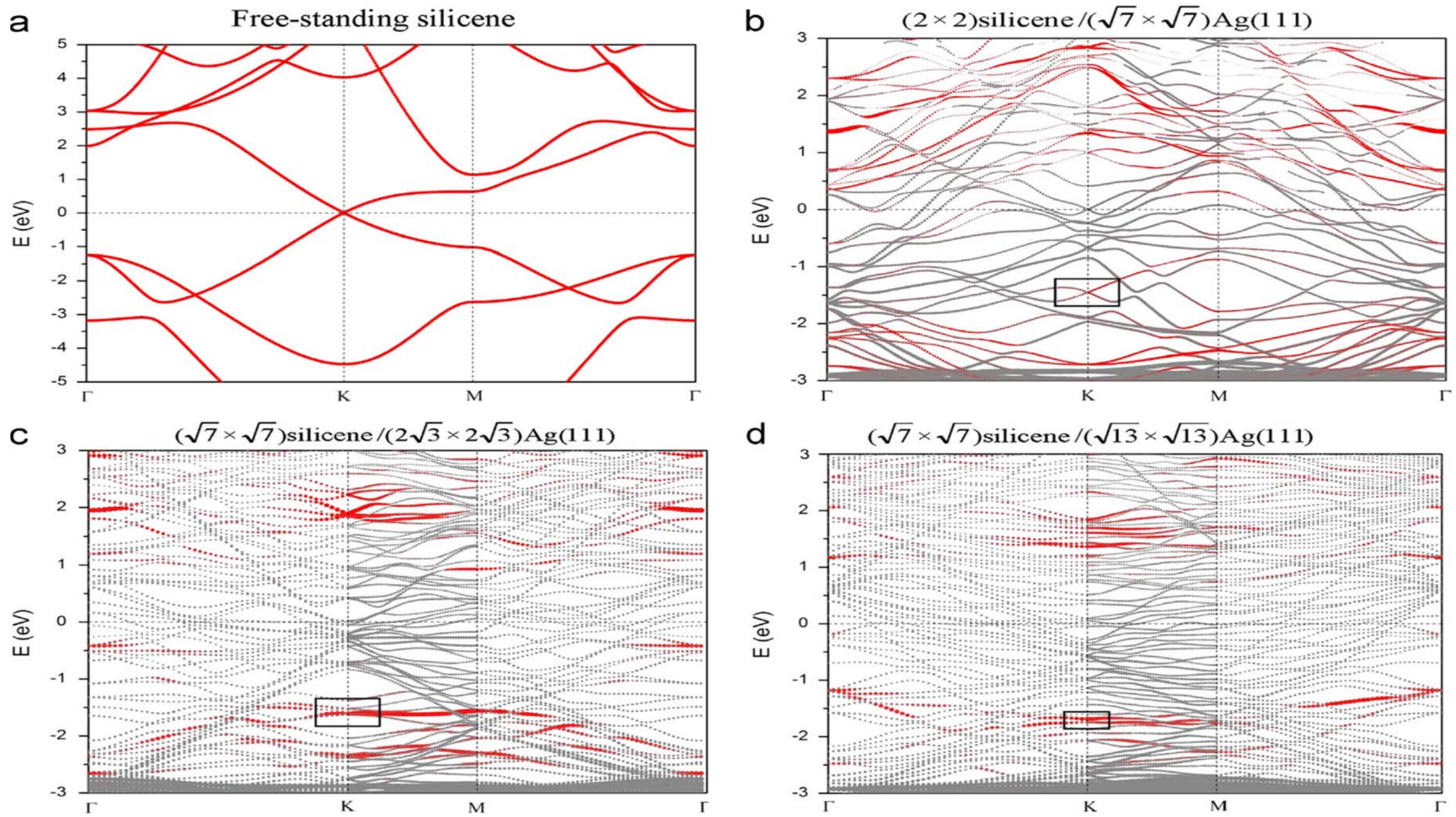

Red line: Silicon compenent

Absence of Dirac cone on ZrB_2 and MoS_2 substrates

Fig. 3: Silicene on ZrB_2:
Phys. Rev. Lett., 108, 245501 (2012).

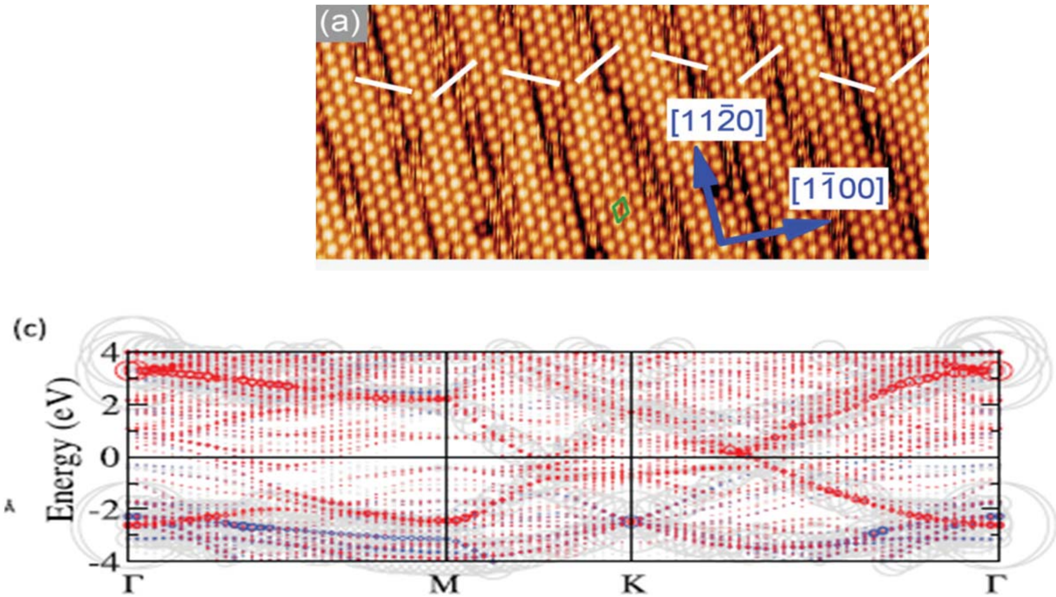

Fig. 4: Silicene on MoS_2
Adv. Mater., 26, 2096-2101 (2014).

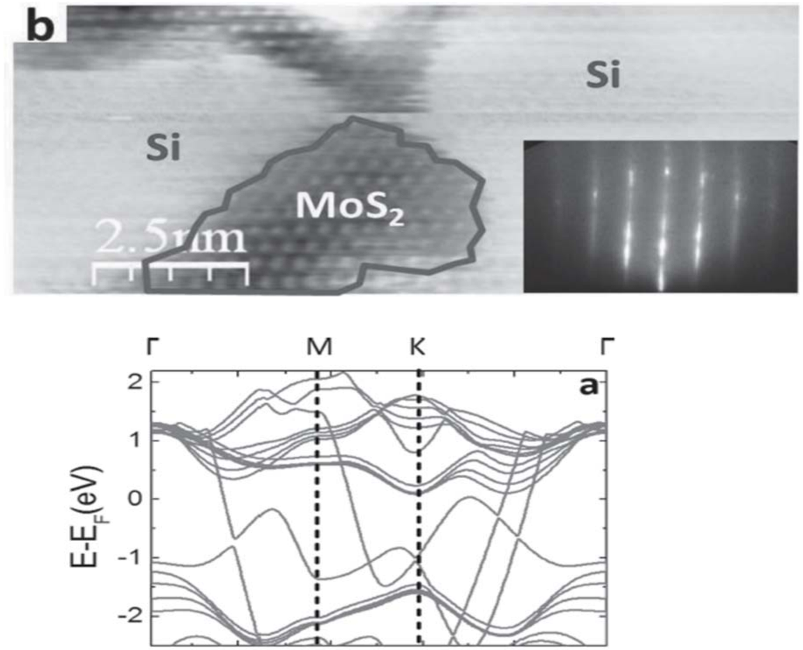

Dirac cone of silicene can be kept on graphene, BN et al
Unsuitable as growth substrate

Question : Is there growth substrate that does not destroy the Dirac cone of silicene?

Ideal novel substrates for silicene growth ——Group III MonoChalcogenide (G3MC)

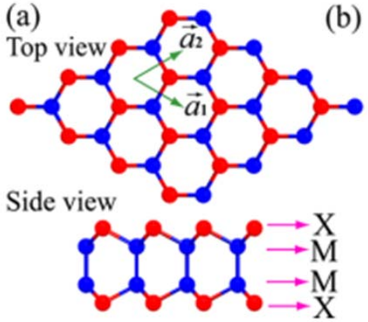

2D G3MC
Lattice constant：3.6~4.3 Å
Silicene：3.8~3.9 Å

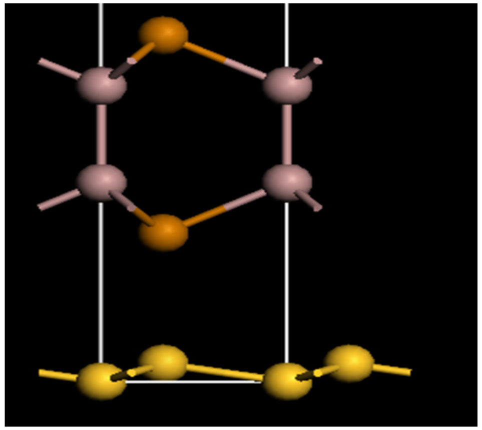

configuration of silicene on G3MC (GaSe)

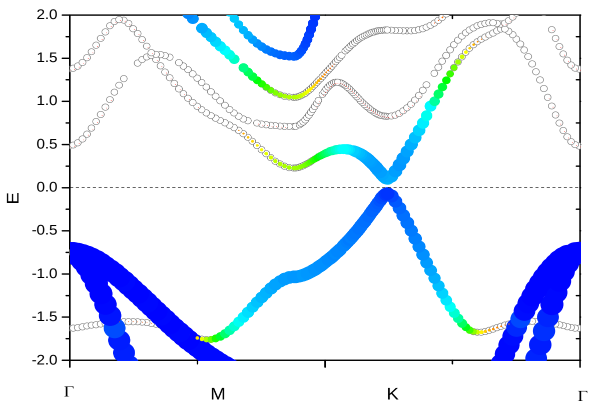

Band structure of silicene on GaSe. The color indicates the projection of Si atoms.

Table 1 Bandgap of silicene on several G3MCs. * indicates indirect bandgap.

G3MC	Gap of silicene E_g (eV)
GaS*	0. 034
GaSe	0.14
GaTe	0.18
InSe	0.14

硅烯FET

硅烯具有极高的载流子迁移率 1×10^{4} $cm^2/V\cdot s$, 能隙0

1. 垂直电场

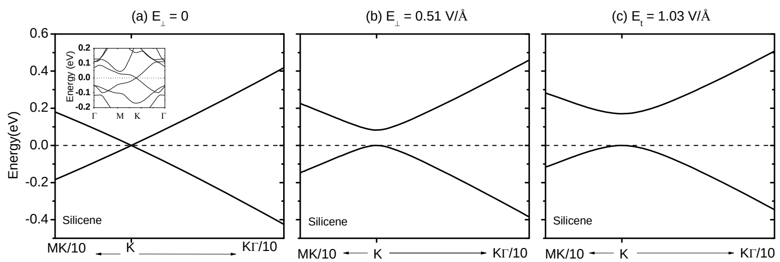

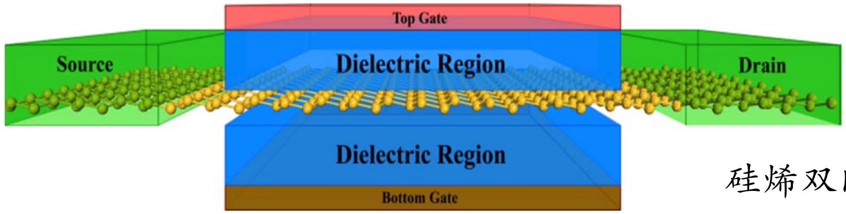

硅烯双门FET

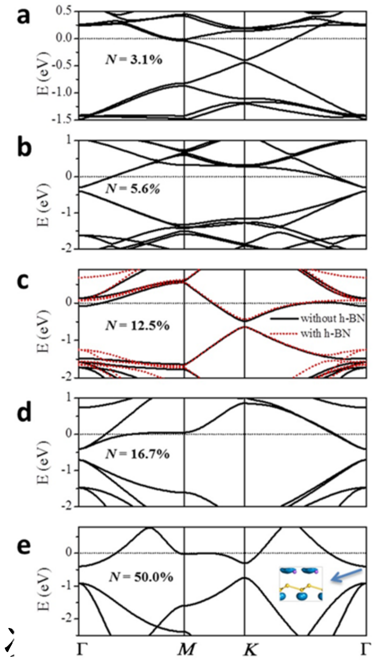

2. 单面吸附

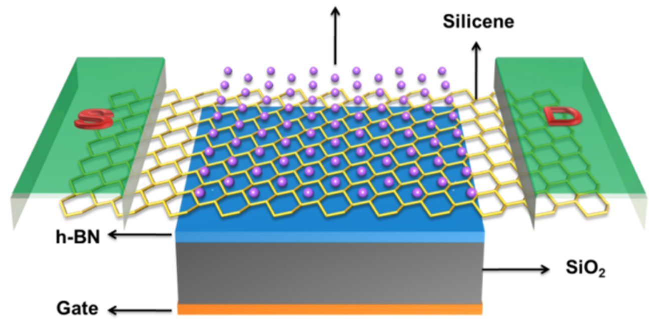

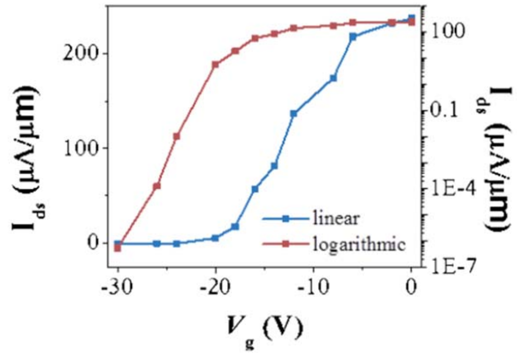

这是国际上最先意识到硅烯具有电场可调能隙

倪泽远 吕劲 Nano Lett 12， 113 （2012），被引200

12/1099

问题：供应电压太大，功耗太大

主要缺点：实验最大电场下能隙太小 0.1 eV

双门

屈贺 吕劲 **Scientific Reports 2：853（201**

47

Silicene Nanomesh

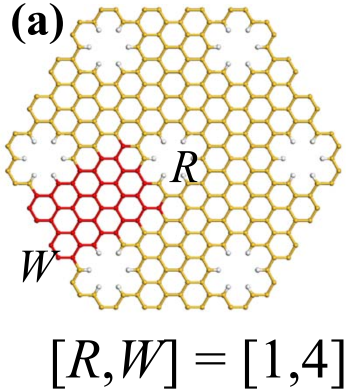

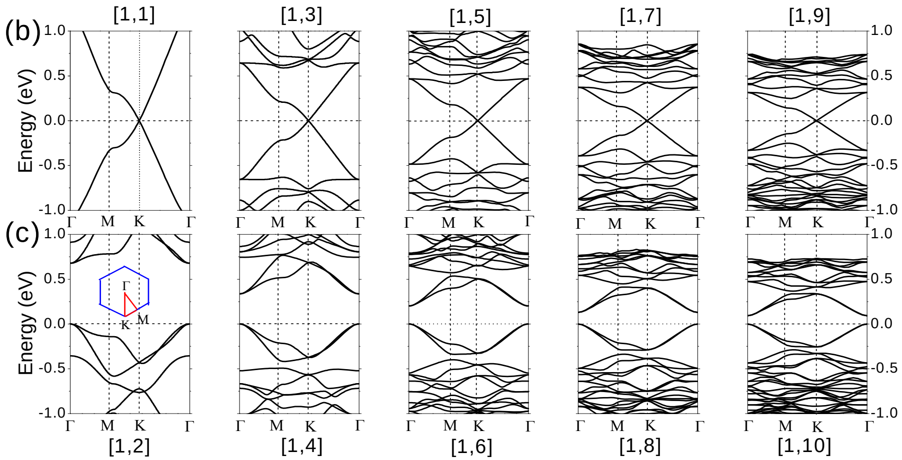

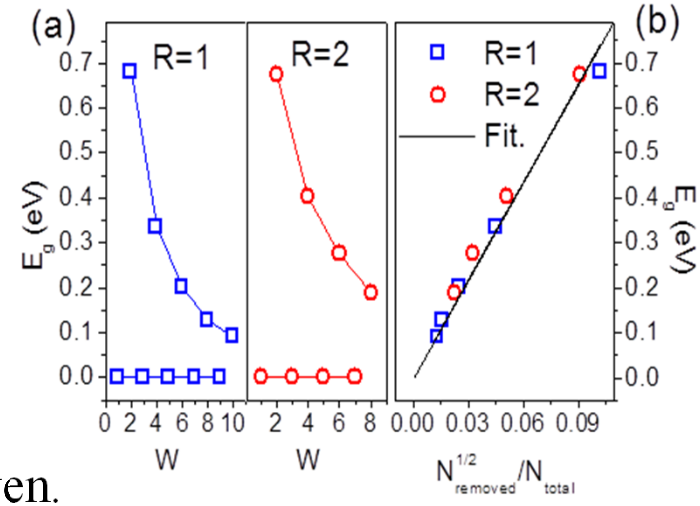

Bandgap of silicene nanomeshes is only opened when *W* is even.

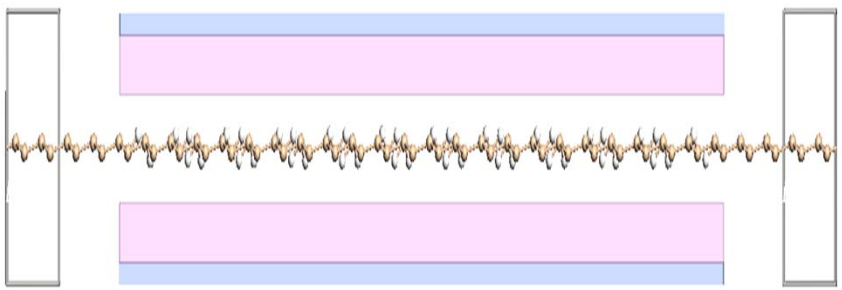

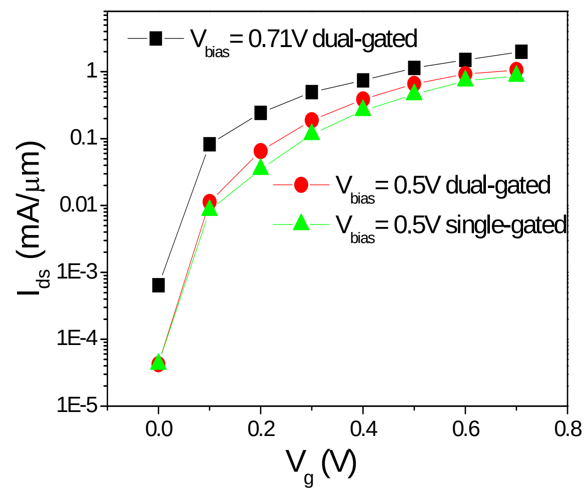

Table Comparison of Performance Metrics Between Sub-10nm Silicene Nanomesh (SNM), Advance Si, carbon nanotube (CNT) Transistors under V_{bias}=0.5V and V_{gate}=0.5V.

Channel	L_{ch} (nm)	I_{on}(μA/μm)	I_{on}/I_{off}	*Subthreshold swing SS* (mV/dec)
SNM dual-gated	7.8	607	1.6×10^4	72
Si nanowire	10	300	1.0×10^4	89 (V_{bias}=1.0V)
Si Fin	10	138	1.0×10^3	125 (V_{bias}=1.2 V)
ETSOI	8	41	1.0×10^4	83 (V_{bias}=1.2 V)
CNT	9	630	1.0×10^4	94

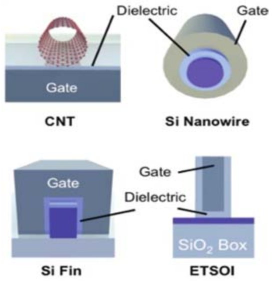

Scientific Reports, in revision

3 石墨炔

研究动机： 石墨炔有高的载流子迁移率(1×10^5 $cm^2/V\cdot s$)

和合适的能隙(0.5 eV (DFT) 1.1 eV (GW)

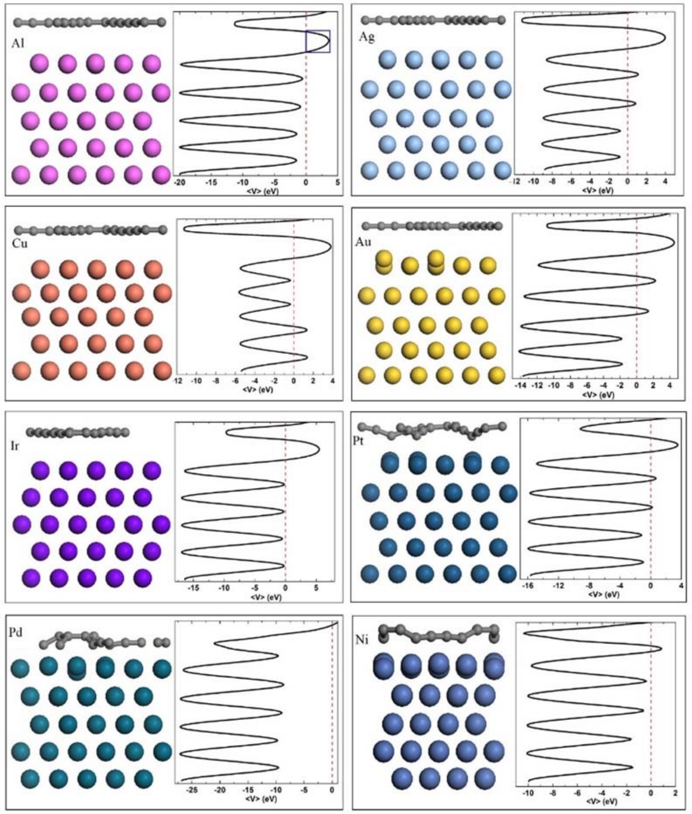

界面结构

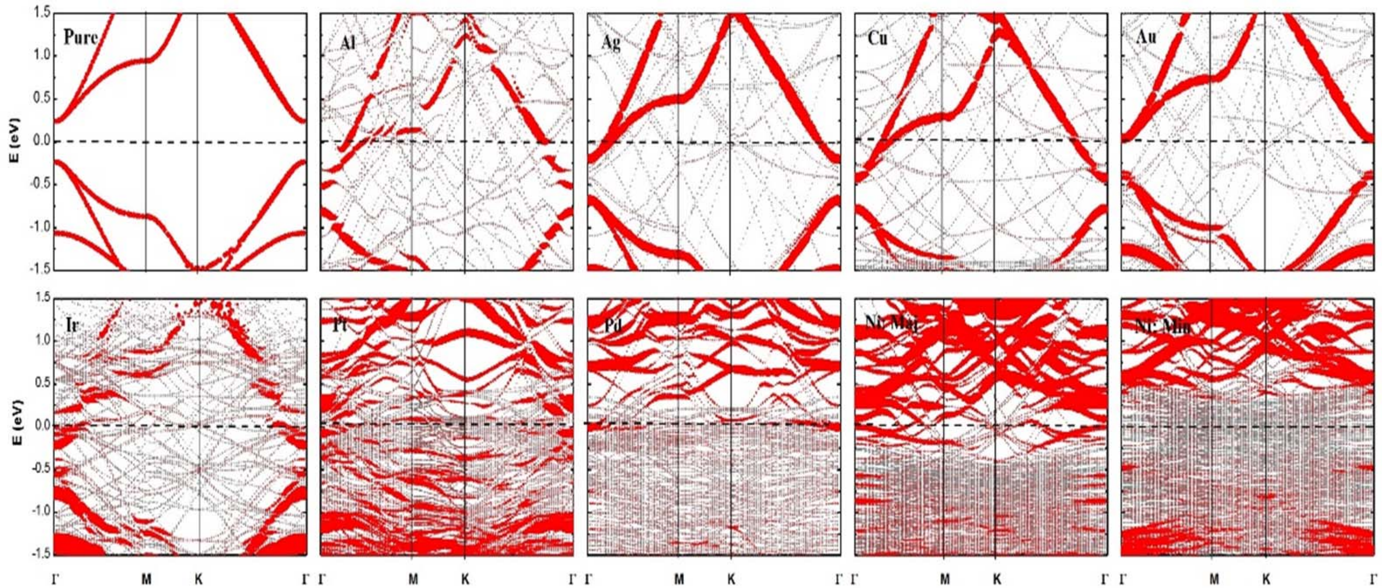

石墨炔与金属接触的能带图

石墨炔FET 界面

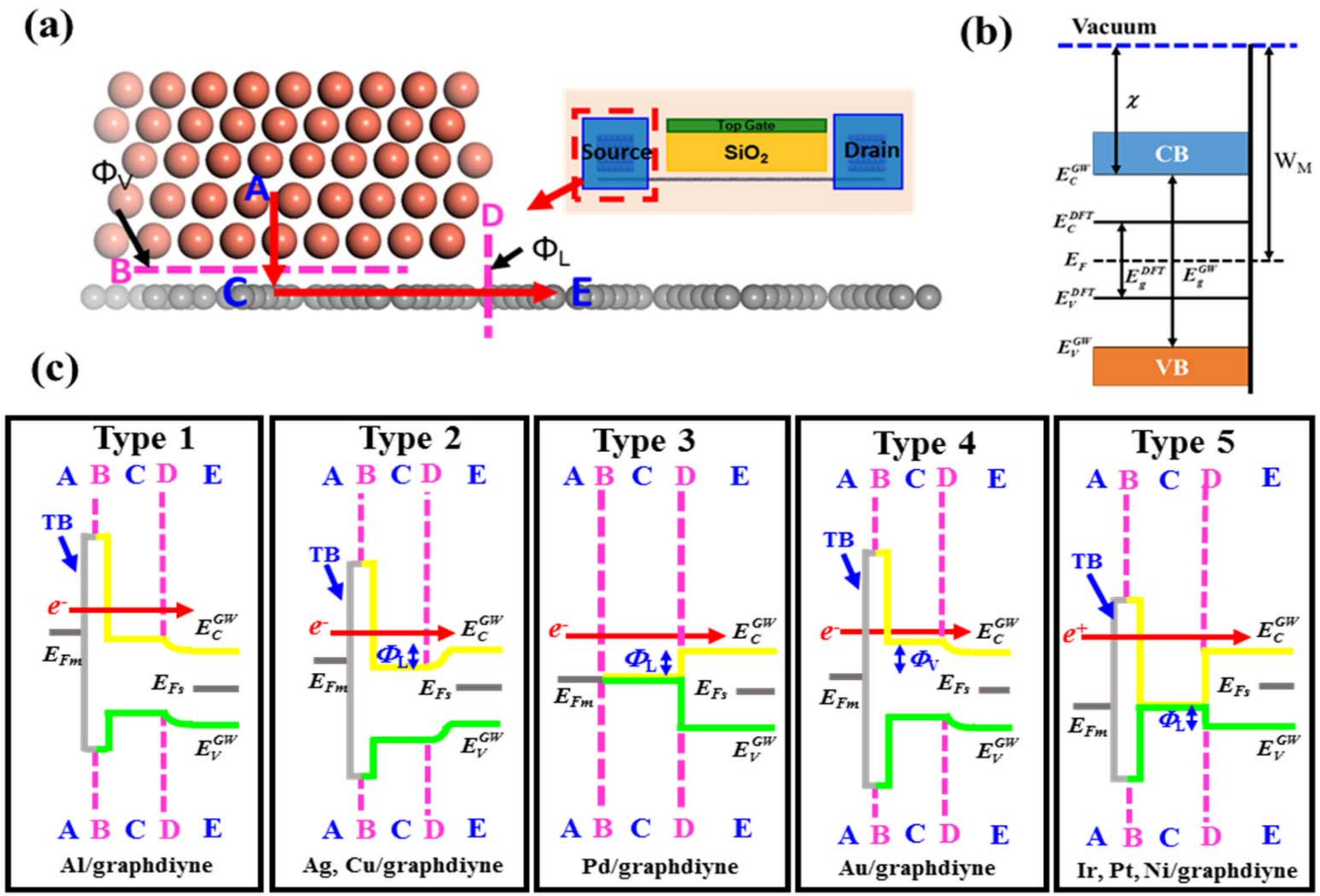

1 Al 欧姆接触 Ag, Cu 准欧姆
其他金属有大的肖特基势垒。

2 Al Ag Cu Pd Au n-type

Ir, Pt, Ni P-type

石墨炔FET

Al

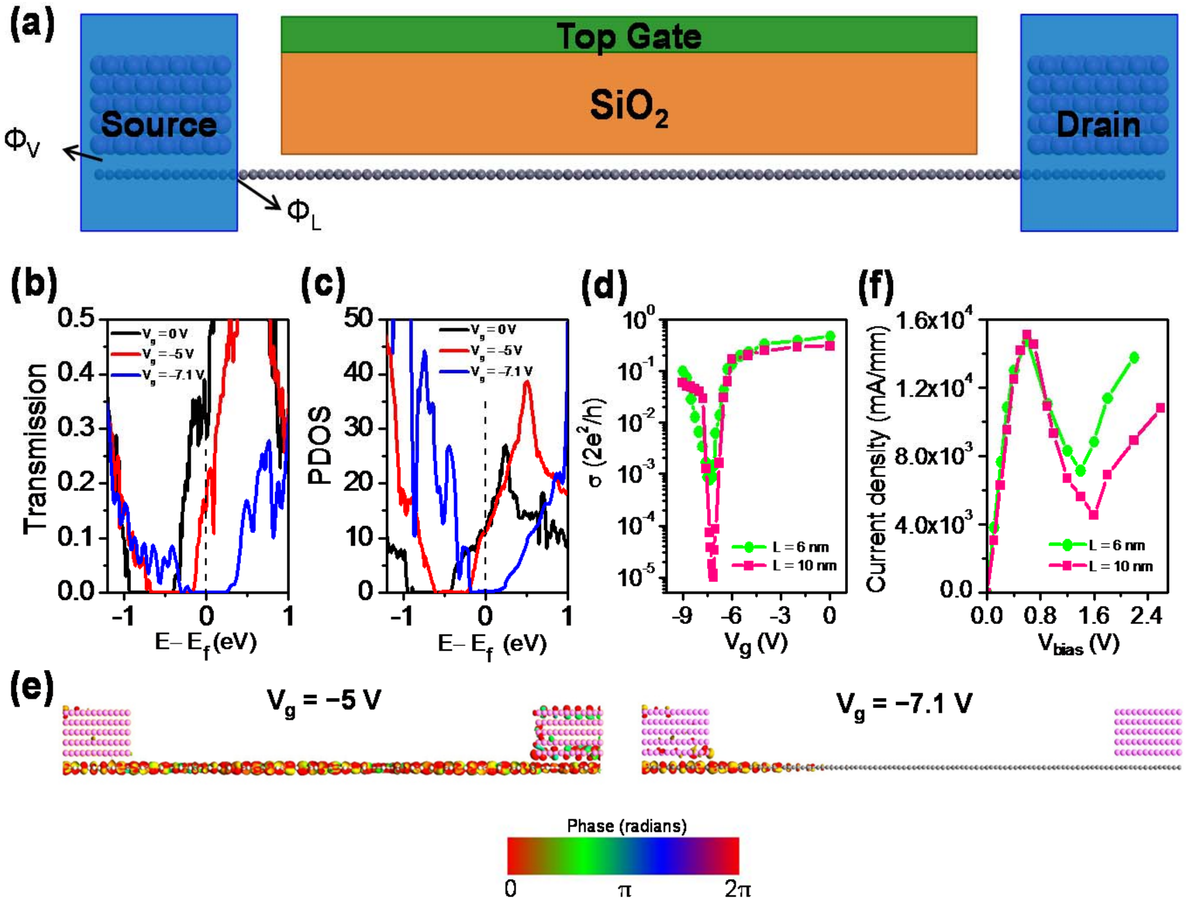

实验

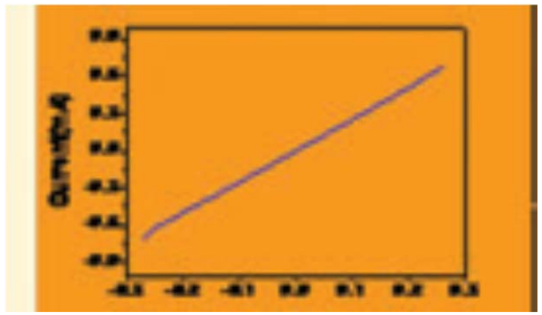

Al, Cu 石墨炔欧姆接触！

李玉良 等 Chem. Commun., 2010, 46, 3256

This device exhibits an on-off ratio up to 10^4 and a sub-threshold swing of 117 mV/dec in a 10 nm channel length.

潘圆圆 王洋洋 吕劲

4 石墨烯 室温载流子迁移率：1.5×10^4 (SiO_2做衬底) — 2×10^5 $cm^2/V\cdot s$ (悬浮)

1 石墨烯三明治

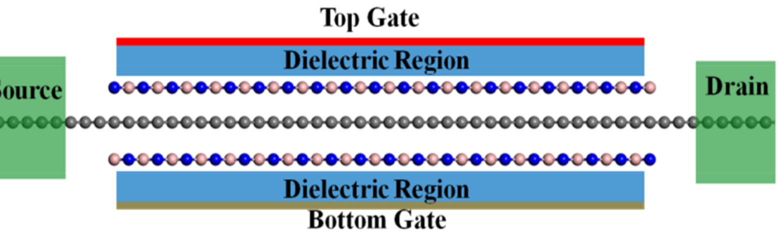

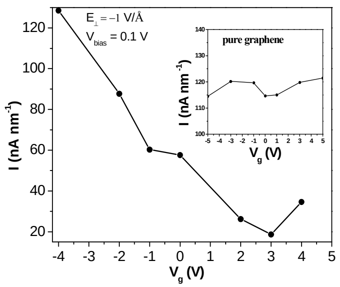

屈贺 吕劲等 被引60 次

NPG Asia Materials (2012) 4, e6; doi:10.1038/am.2012.10

www.nature.com/am

问题： 能隙不超过0.4 eV

2 原子单面吸附

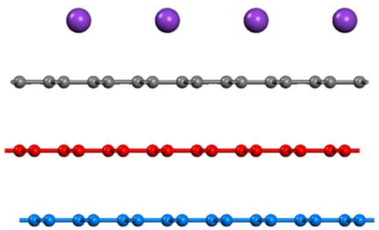

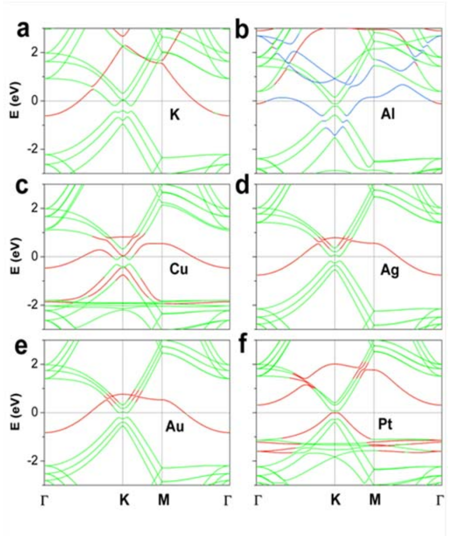

屈贺 吕劲等

Scientific Reports 3, 1794 (2013)

3 与金属接触

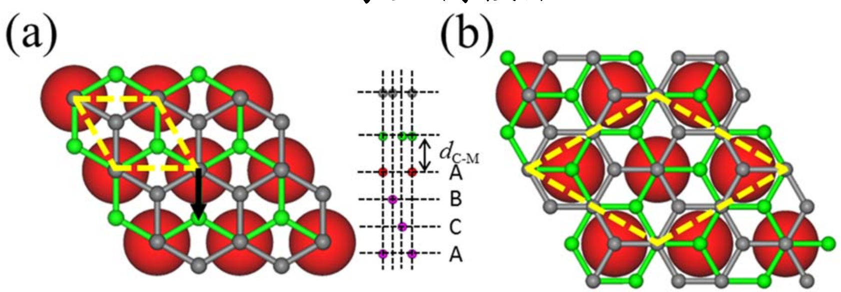

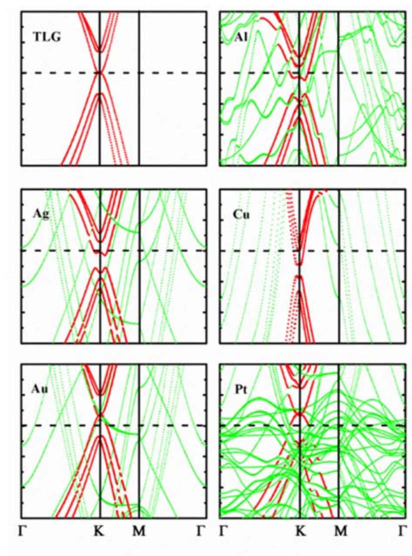

郑家新 王洋洋 吕劲

Scientific Reports 3, 2081 (2013);

石墨烯与硅烯垂直结构FET

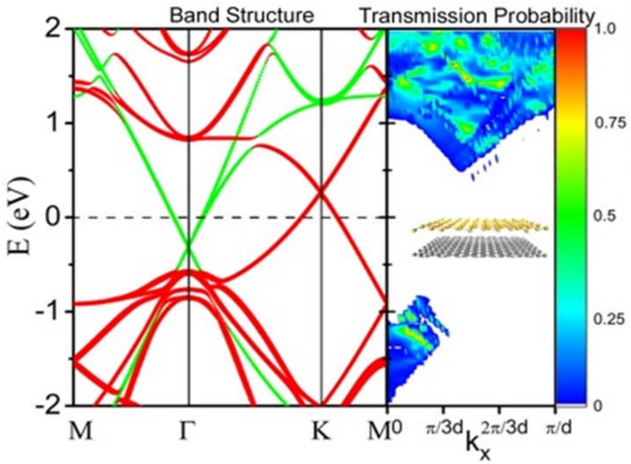

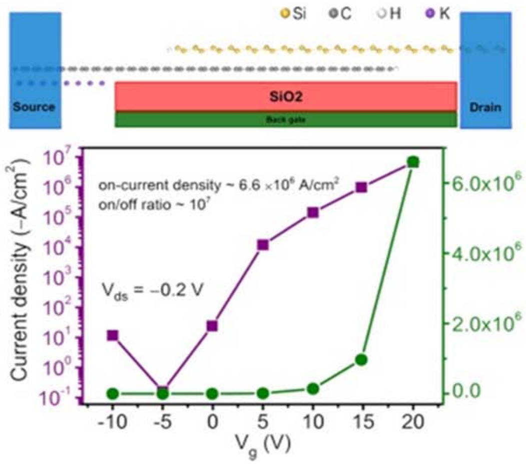

能隙 1.3 eV

开关比 10^7

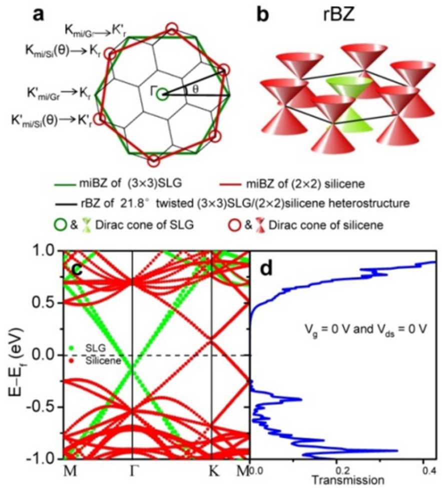

旋转不变能隙

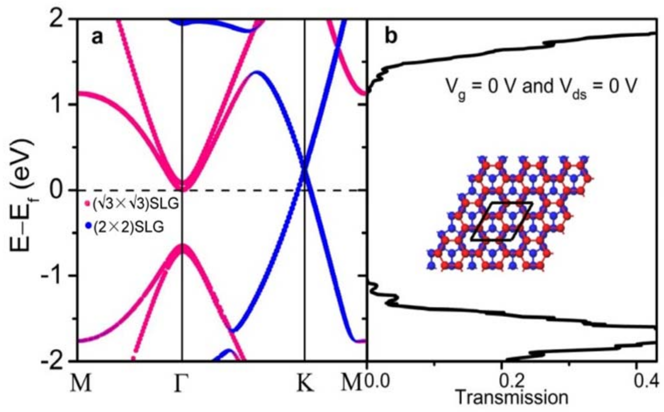

旋转的石墨烯双层能隙存在

全金属

All-metallic FET

不需要打开能隙

利用不同层的狄拉克锥

之间迁移禁止的特点

王洋洋 吕劲 等 **Advanced Functional Materials, in press**

nature nanotechnology LETTERS
PUBLISHED ONLINE: 7 SEPTEMBER 2014 | DOI: 10.1038/NNANO.2014.187

Twist-controlled resonant tunnelling in graphene/boron nitride/graphene heterostructures

A. Mishchenko[1], J. S. Tu[2], Y. Cao[2], R. V. Gorbachev[2], J. R. Wallbank[3], M. T. Greenaway[4], V. E. Morozov[1], S. V. Morozov[5], M. J. Zhu[1], S. L. Wong[1], F. Withers[1], C. R. Woods[1], Y-J. Kim[2,6], K. Watanabe[7], T. Taniguchi[7], E. E. Vdovin[4,5], O. Makarovsky[4], T. M. Fromhold[4], V. I. Fal'ko[3], A. K. Geim[1,2], L. Eaves[1,4] and K. S. Novoselov[1]*

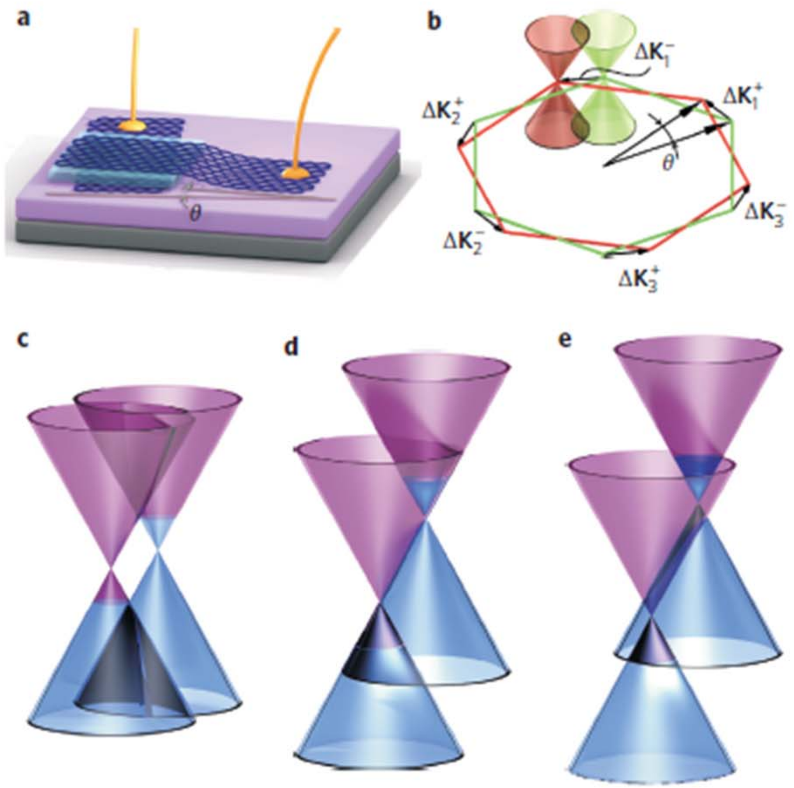

Figure 1 | Schematic representation of our device and its band structure.

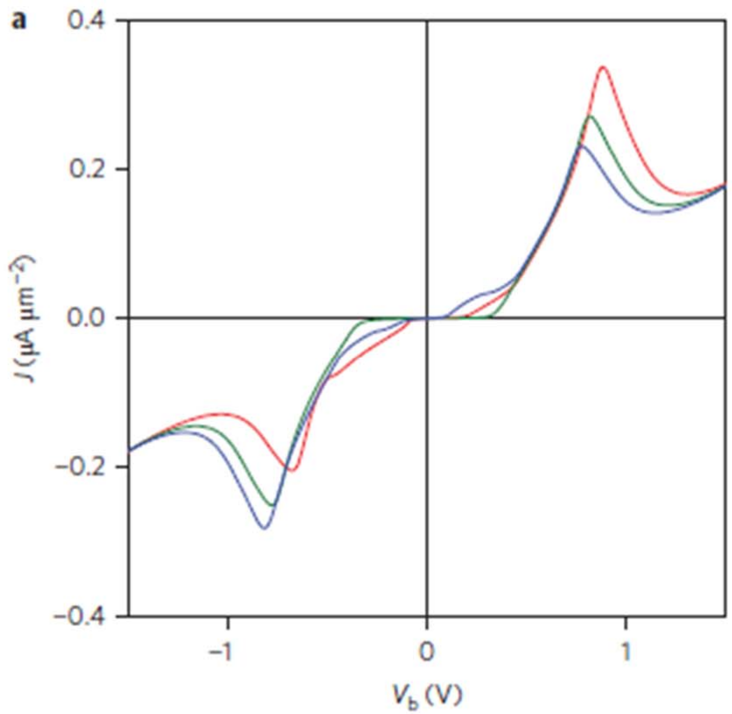

NANO LETTERS
Letter
pubs.acs.org/NanoLett

Tailoring the Electronic Structure in Bilayer Molybdenum Disulfide via Interlayer Twist

Arend M. van der Zande,[†,‡,*] Jens Kunstmann,[†,§] Alexey Chernikov,[∥] Daniel A. Chenet,[‡] YuMeng You,[∥] XiaoXiao Zhang,[∥] Pinshane Y. Huang,[⊥] Timothy C. Berkelbach,[†,§] Lei Wang,[‡] Fan Zhang,[‡] Mark S. Hybertsen,[†,#] David A. Muller,[⊥,¶] David R. Reichman,[†,∥] Tony F. Heinz,[†,∥] and James C. Hone[†,‡]

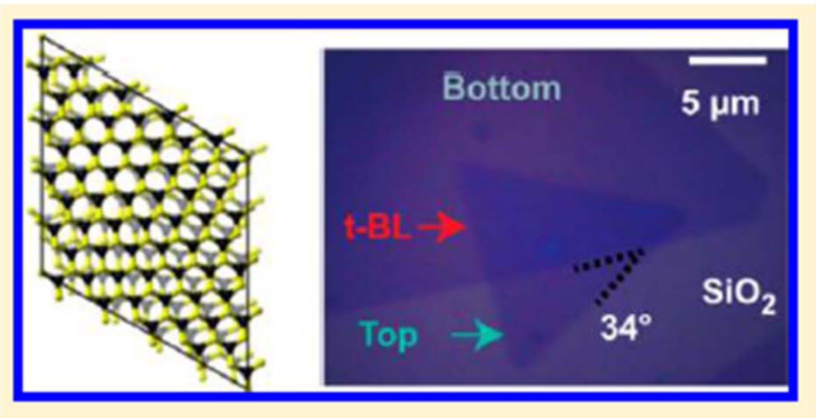

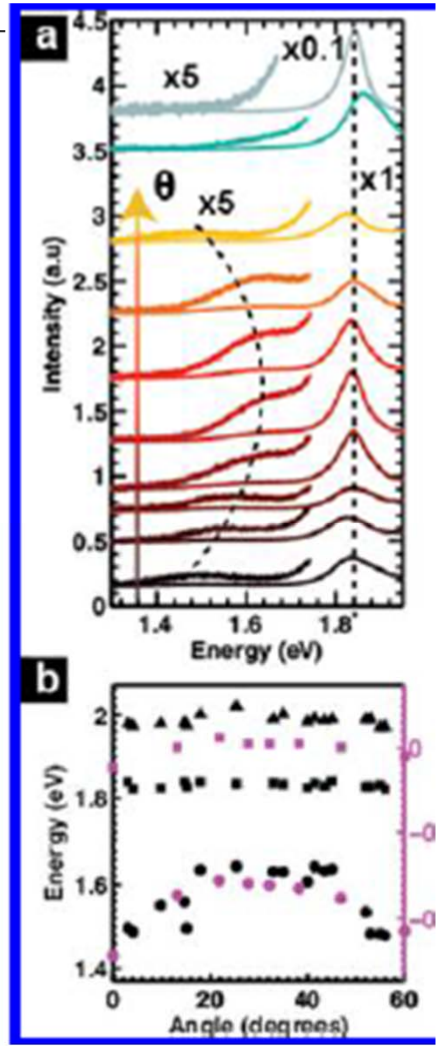

双层的MoS2 旋转后可以观察到圆偏振光的选择性

黑磷

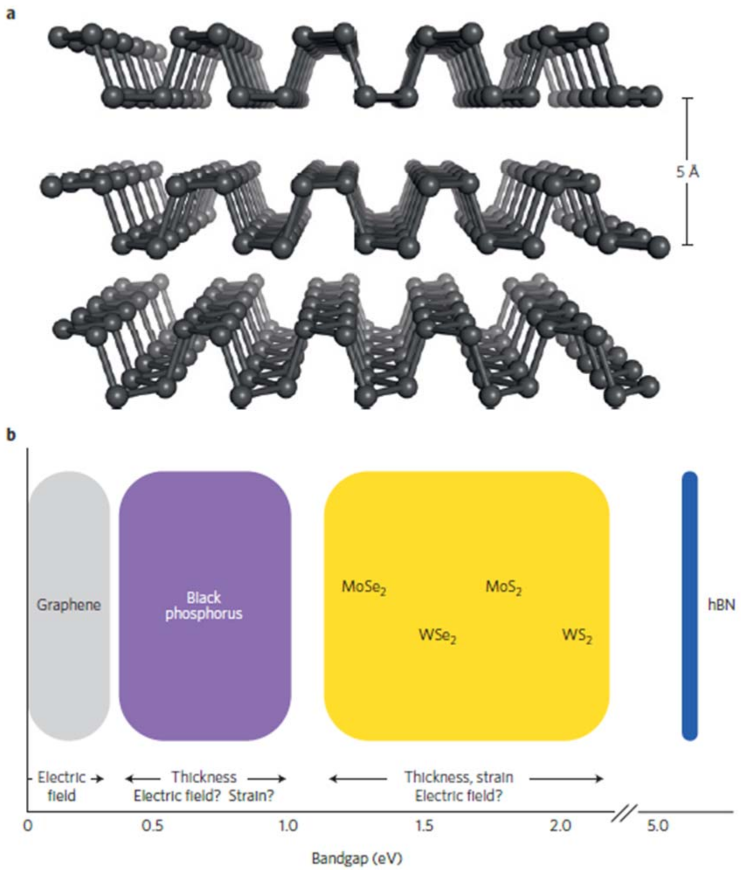

Figure 1 | Black phosphorus structure and bandgaps of layered materials. **a**, The layered and anisotropic crystal structure of elemental black phosphorus. **b**, Bandgap energies of several layered materials used for nanoelectronics. The range of values for each material can be achieved through a variety of means. For example, it is expected that variations in an applied perpendicular electric field, film thickness or strain could modify the bandgap value. hBN, hexagonal boron nitride.

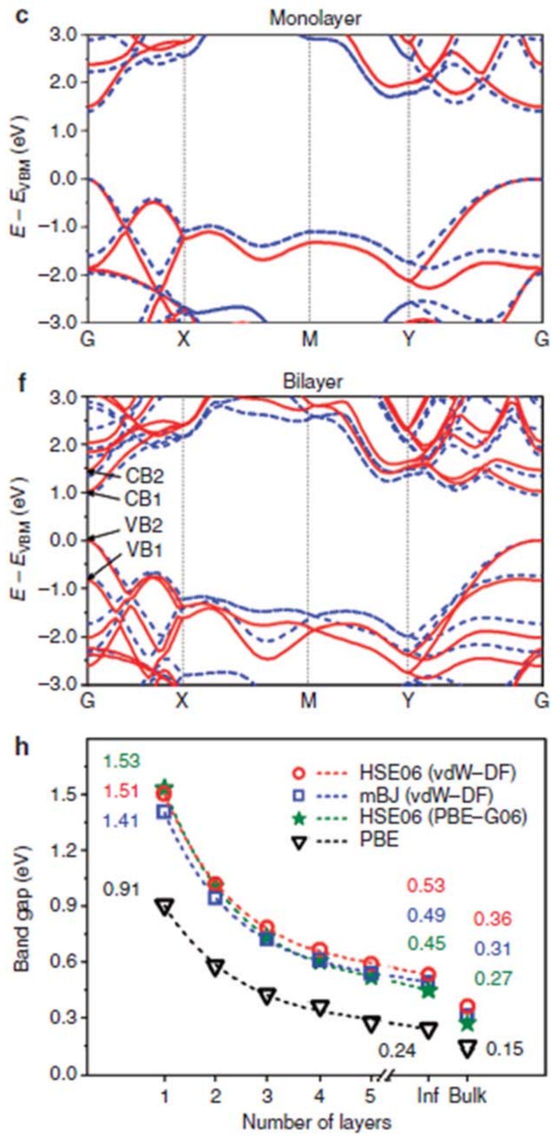

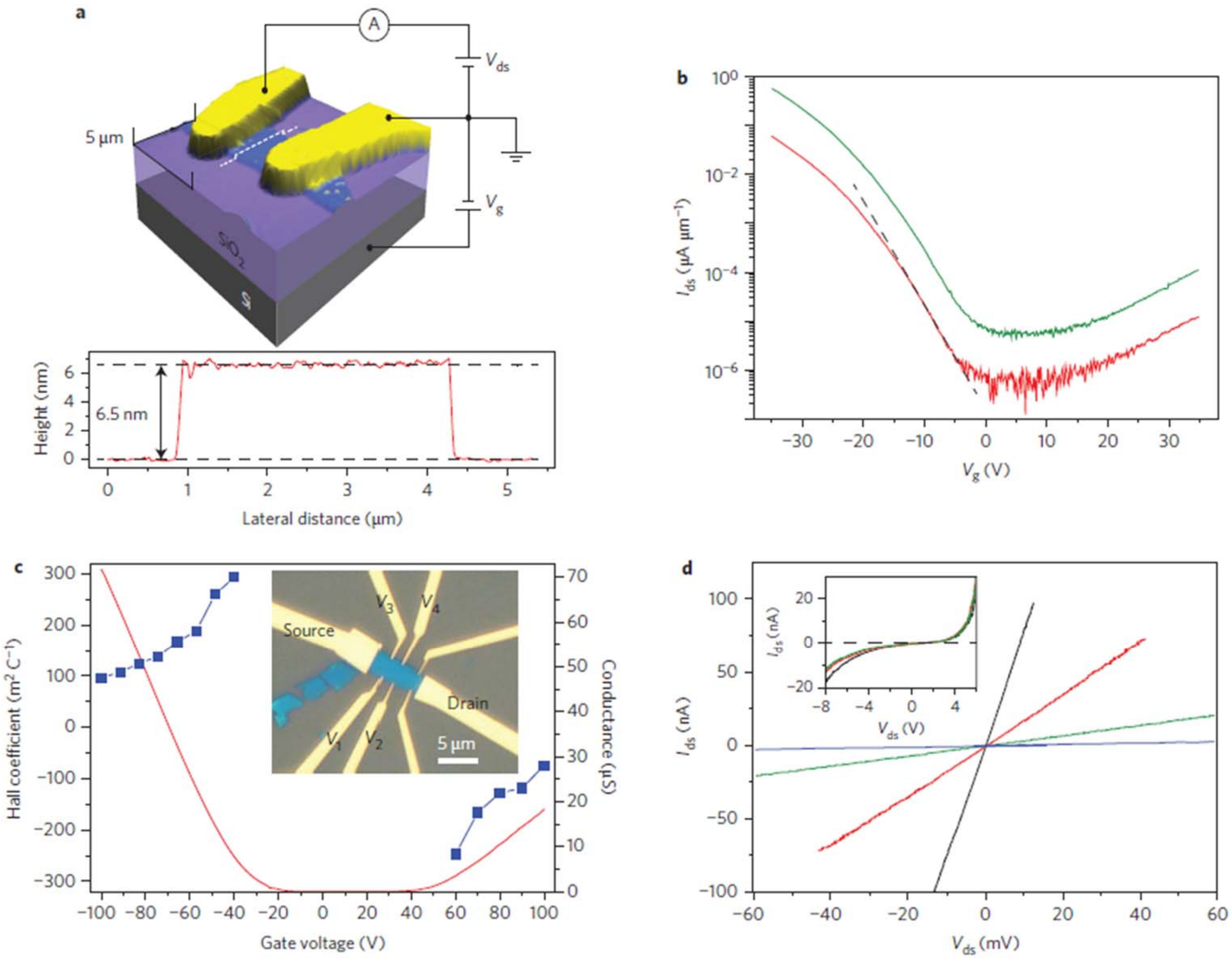

nature nanotechnology
ARTICLES
PUBLISHED ONLINE: 2 MARCH 2014 | DOI: 10.1038/NNANO.2014.35

Black phosphorus field-effect transistors

Likai Li[1], Yijun Yu[1], Guo Jun Ye[2], Qingqin Ge[1], Xuedong Ou[1], Hua Wu[1], Donglai Feng[1], Xian Hui Chen[2]* and Yuanbo Zhang[1]*

Black Phosphorus-Monolayer MoS_2 van der Waals Heterojunction p-n Diode[1]

1. Deng, Y. *et al. ACS Nano* **8**, 8292–8299 (2014).

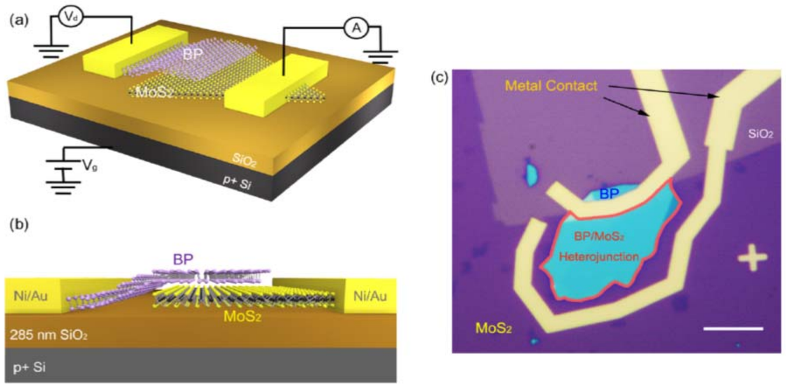

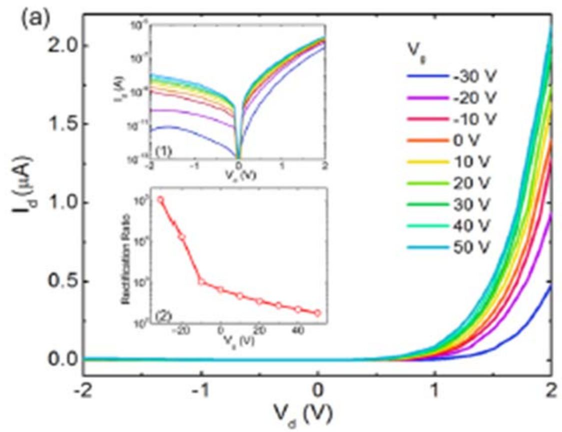

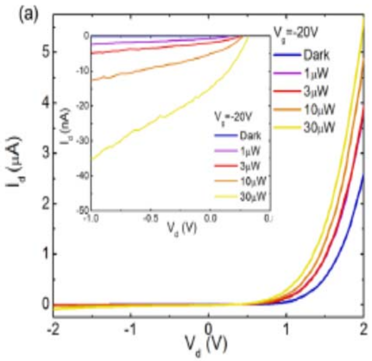

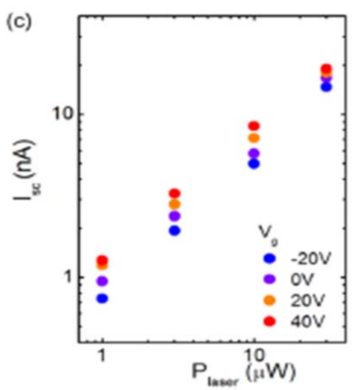

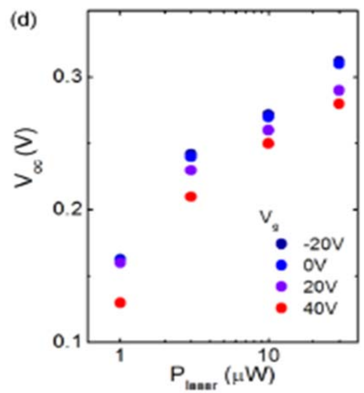

可能发展:

1　门的控制p-n 结

2　同质的材料

I_{sc} as a

function of laser power under different back gate voltage. (d) V_{oc} as a function of laser power under different back gate voltage. Increasing the back gate voltage increases I_{sc} but reduces V_{oc}.

总结

1　多体效应可期待在更多的MX2上观测。衬底的影响值得进一步研究。

2　MoS_2还可以满足ITRS 10 nm 器件的要求。可以继续缩小FET。

3　光电器件可以进一步简化。努力实现TFET.

4　谷电子学-自旋电子学耦合在一起，显示了丰富的物理。
双层MoS2 的谷霍尔效应应该在加垂直电场时候可以实现。

5 自旋流尚待测观。谷轨道磁矩流和霍尔效应也应存在.

6 层间旋转会带来新的调控。

致谢

基金委　科技部 教育部

合作者：　史俊杰，杨金波，俞大鹏，李巨（MIT），杨李（华盛顿）

Ph. D candidates:

宋志刚

王洋洋

屈贺如歌

倪泽远 Ni Zeyuan

潘圆圆

钟红霞　潘峰